2020

Establishing a Myocardial Ischemia-Reperfusion Injury Model in Mice and Rats using Left Anterior Descending Artery Ligation and Isolated Heart Experiments

Alexander Papa
Philadelphia College of Osteopathic Medicine

Philadelphia College of Osteopathic Medicine
Graduate Program in Biomedical Sciences
Department of Bio-Medical Sciences

Establishing a Myocardial Ischemia-Reperfusion Injury model in mice and rats using Left Anterior Descending Artery ligation and Isolated Heart experiments.

A Thesis in Biomedical Sciences by Alexander Papa

We, the undersigned, duly appointed committee have read and examined this manuscript and certify it is adequate in scope and quality as a thesis for this master's degree. We approve the content of the thesis to be submitted for processing and acceptance.

_____

Qian Chen, PhD, Thesis Advisor
Assistant Professor of Physiology and Pharmacology
Department of Bio-Medical Sciences

_____

Cathy J. Hatcher, PhD, Thesis Committee Member
Associate Professor of Neuroscience, Physiology and Pharmacology
Department of Bio-Medical Sciences

_____

Bohdan Minczak, M.D., Thesis Committee Member
Department of Bio-Medical Sciences

TABLE OF CONTENTS

I. ABSTRACT

Myocardial infarction (MI) is a leading cause of death globally, with over 730,000 cases each year in the United States alone. Factors involved in the prognosis of an MI include identification of the artery occluded, the time to reperfusion, the size of the infarct, and the degree of cardiomyocyte death. Thus, the treatment of MI typically involves targeting one or more of these factors. Timely opening of an occluded artery to reperfuse the ischemic tissue remains the mainstay treatment through either thrombolytic therapy, arterial stenting, or percutaneous coronary intervention. However, reperfusion itself may cause further damage through the generation of reactive oxygen species (ROS) in a process known as myocardial ischemia-reperfusion injury. There are no clinically accepted treatments that directly target cardiomyocyte reperfusion injuries, and the pathophysiology of the process remains complex. Due to the high mortality, lack of positive clinical evidence, and complex pathophysiology, it is difficult to safely measure and study MIR injuries in humans. However, parallel animal models that mimic infarctions in an experimental setting will be essential in furthering the understanding and treatment for MIR injuries. In order to progress research in the field of MIR injury, a reliable and reproducible study model must first be established. The goal of the study is to establish two different models of MIR injury and provide positive evidence that they are reproducible, effective, and reliable. The first model will establish an in vivo Left Anterior Descending (LAD) artery ligation model in mice, which will result in an MIR injury observable through ECG changes and through obtaining a percentage of infarction. The second model will establish a Langendorff model that will show similar cardiomyocyte death, measurable through changes to LVESP, LVEDP, dPTd max, dP/dT min, heart rate and coronary flow, and by obtaining a percentage of infarction. We found that, iIn summary, both models showed evidence of MIR

injury confirmable through ECG changes, tissue staining, and cardiac function and coronary flow reduction.

II. INTRODUCTION

2.1 Myocardial Infarction

Myocardial infarction (MI) continues to be a major cause of mortality, with 840,000 deaths in the United States per year and 17.6 million worldwide (AHA). The annual healthcare costs of cardiovascular disease also continue to grow, with an estimated $350 billion dollars spent in hospital fees in the United States alone. Risk factors for MI are extensive, including tobacco use, physical activity, obesity, diabetes, and high cholesterol.

Acute myocardial infarction is not always the cause of death. Instead, infarct progresses to weakened contractile ability of the heart, known as heart failure. Heart failure may manifest into various clinical effects, such as edema, hypotension, syncope, and arrhythmias. All of these increase the risk of death, increase healthcare costs, and cause distressing symptoms. The size of infarct is shown to be a strong predictor of clinical prognosis post-MI, even more so than measuring LV ejection fraction or contractility [*Kelle et a., 2009.*]. Thus, reducing the size of infarct and preserving viable tissue is the primary goal in treatment of an MI.

2.2 Ischemia Reperfusion Injury

In order to preserve viable tissue, primary treatment of an acute infarct involves prompt restoration of blood flow in the occluded vessel through primary percutaneous coronary intervention and fibrinolytic drugs. Paradoxically, reperfusion of the ischemic tissue can cause additional tissue damage in a process known as myocardial ischemia reperfusion injury (MIR), and may account for up to 50% of the final size of the infarct [*Yellon et al., 2007*]. Despite many promising preclinical trials targeting MIR, none have proved successful clinically. Thus, limiting reperfusion injury remains to be a highly active area of cardiac research.

One major cause of injury in MIR is due to the generation of highly reactive elements called free radicals (e.g. reactive oxygen species), which ultimately cause damage through direct cellular injury [*Garcia-Dorado et al., 2009]*. Mechanisms leading up to the initial generation of ROS are not completely clear. One proposed mechanism is the production of ROS is actually multifactorial, and may involve: 1. changes in levels of Nitric Oxide (NO), which serves as a potent vasodilator; 2. reductions in pH, which serve as a catalyst for enzymatic reactions; and 3. reduction of ATP generation due to loss of aerobic respiration in the mitochondria. These factors promote the upregulation of enzymes that are capable of ROS generation once oxygen is re-introduced, and include Xanthine Oxidase and NADPH oxidase. Free radicals are also generated by the mitochondria, but are normally contained within the mitochondria. However, when the electron transport chain is uncoupled due to an ischemia-reperfusion injury, more electrons will leak out and produce superoxide more than antioxidant capacity in the mitochondria. When the membrane permeability is damaged, mitochondrial free radicals may leak into the cytosol. Newly generated free radicals, such as superoxide (O2-), hydrogen peroxide (H2O2), and hydroxyl radical (OH), interact violently with lipids expressed within the cell membrane of cardiomyocytes, stripping them from their membrane in a process called peroxidation. This removal causes the formation of pores within the cell membrane, allowing cell contents to leak and ultimately causing cell death [*Yellon et al., 2007]*.

Reperfusion injury is further complicated by the eventual release of pro-inflammatory cytokines and arachidonic acid from the dying cells. Cytokines, such as tumor necrosis factor, induce inflammatory changes and cause the migration of immunologic cells, such as neutrophils and macrophages, degrading viable tissue further. Arachidonic acid is responsible for the downstream formation of leukotrienes, prostaglandins, and thromboxane A2, all of which may

also mediate an influx of immunologic and inflammatory cells. Damaged cells may also release stored calcium, which is a potent mediator of cardiomyocyte contraction. [*Neri et al., 2007*].The sudden calcium influx causes a phenomenon called contraction band necrosis - due to the hypercontraction of the cells and lack of a relaxation signal. The overwhelming generation of ROS may interact with cell mitochondria by promoting the opening of mitochondrial permeability transition pores (MPTP), which are important for maintaining mitochondrial membrane potential. Disruption of this membrane causes cellular lysis and swelling, as well as further generation of ROS. Finally, damage to the mitochondria may allow the release of pro-apoptotic factors into the cytosol, such as Cytochrome C, which may promote further cell death and potentiate the cycle of ROS generation. [Sang-Bing Ong et al., 2014]There are a multitude of other factors involved in reperfusion injuries, each interacting with one another in a way that can permeate further damage, but the initial mediator of this damage is theorized to be the generation of reactive oxygen species.

2.3 The clinical manifestations of heart ischemia

2.3.1 ECG Changes

Clinically, transient heart ischemia presents with a multitude of observable and testable findings. These findings range from clinical exam findings, such as diffuse chest pain, to testable findings, such as ECG changes and rises in blood Troponin levels. Testing for confirmation of ischemic heart disease usually begins with an ECG, as it is fast and changes can usually be seen within seconds to minutes of the beginning of an ischemic event. Common ECG findings in a myocardial infarction include heart rate changes, ST segment elevations, Q wave changes, and T wave inversions.

In a healthy heart, and ECG tracing will usually include a P wave, QRS complex, and T wave (*figure 1*). These separate waveforms represent electrical conduction by the heart, which is then translated to a waveform pattern on an ECG monitor which measures the amplitude of the contraction in millivolts. The size, shape, and length of these waveforms will differentiate the type of contraction and the time of the heart cycle.

The "P" wave represents the depolarization of the atria as the electrical impulse of the heart travels from the Sinoatrial (SA) node to Atrioventricular node (AV) and Bundle of His. During atrial contraction, blood is flowing from the left and right atria into the left and right ventricles, respectively. This period of time is known as diastole, where blood fills the ventricular space in order to prepare for ejection into the pulmonary vasculature or systemic vasculature. P wave changes may occur in myocardial infarction involving the atria, which may present as an elevation of 1mm or more in leads V1-V2 of a 12-lead ECG. [CVPhysiology]

The QRS complex represents ventricular depolarization, or the ejection period of a normal heart cycle. Typically, the QRS complex is narrow and depolarization happens quickly, within 0.10 seconds in a healthy heart. Changes to the width of the QRS complex, or the time for depolarization, may occur in MI due to the inability of ischemic or infarcted tissue to conduct a depolarization properly.

The T wave is typically the final waveform in a healthy heart, and represents the repolarization of the ventricle. At this time in a normal cardiac cycle, the heart has ejected blood from the ventricular cavities and has completed systole, and diastole has now begun.

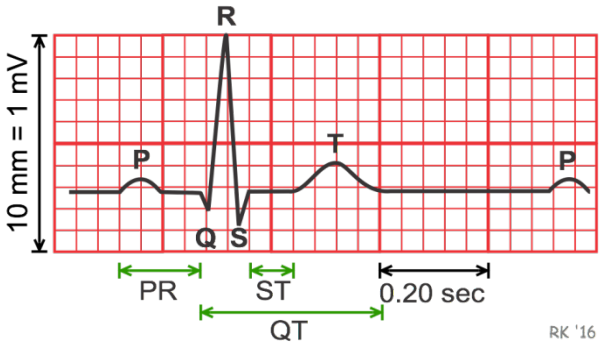

Figure 1. This schematic representation shows a normal ECG tracing from a complete heart cycle. Various ECG waveforms and segments are depicted here and are described in detail above. (Source: Plus PNG EKG Images)

The use of the ECG, particularly the 12-lead ECG, has become a necessity in quick diagnosis of myocardial infarctions due to its high specificity and immediate changes following heart ischemia (*Figure 2)*. While measuring blood Troponins or CK-MB are also useful and specific, these cardiac markers typically do not rise until at least 30 minutes after onset of ischemia, making the ECG the best diagnostic tool for early emergency diagnosis of heart ischemia [*Achar et al., 2005*.

Typically, the most obvious change in a myocardial infarction is changes to the ST-segment, measured by the difference in the "J" point. The location of the ST-segment changes on a 12-lead ECG, as well as changes in the amplitude of the ST-segment, may help diagnose cardiac ischemia. It may also help to identify the exact location of the ischemia on the heart, as well as if the ischemia is due to a transmural or non-transmural ischemic injury. Typically, an ST elevation measured from the J point that is greater than 0.2 mV is evidence of an acute ischemic change. Typically transmural infarctions, usually resulting from total coronary occlusion, are more likely to be associated with ST-elevations. ST segment depressions may also correspond with ischemia, but most often represent non-total occlusions, such as angina due to coronary atherosclerotic

heart disease, where the total luminal diameter of the coronary arteries is significantly reduced, but not obstructed entirely. The location of ST changes on a 12-lead ECG may also aid in diagnosing the location of the ischemia. For example, isolated ST-elevations in heart leads II, III, and aVF will likely represent an occlusion to the inferior wall of the heart, which is usually supplied by the right coronary artery. ST elevations in V1-V6 are typically more specific to the anterior and lateral wall of the heart, supplied primarily by the left anterior descending artery and the circumflex artery.

Other evidence of myocardial ischemia, such as pathologic "Q" waves and T-wave inversions, may also be seen. These waves typically present after ST-segment changes, and are present due to abnormalities in electrical conduction in a portion of the heart that has suffered from ischemia or infarct. These waves, while not diagnostic, are useful as supporting evidence for diagnosing ischemia and myocardial damage.

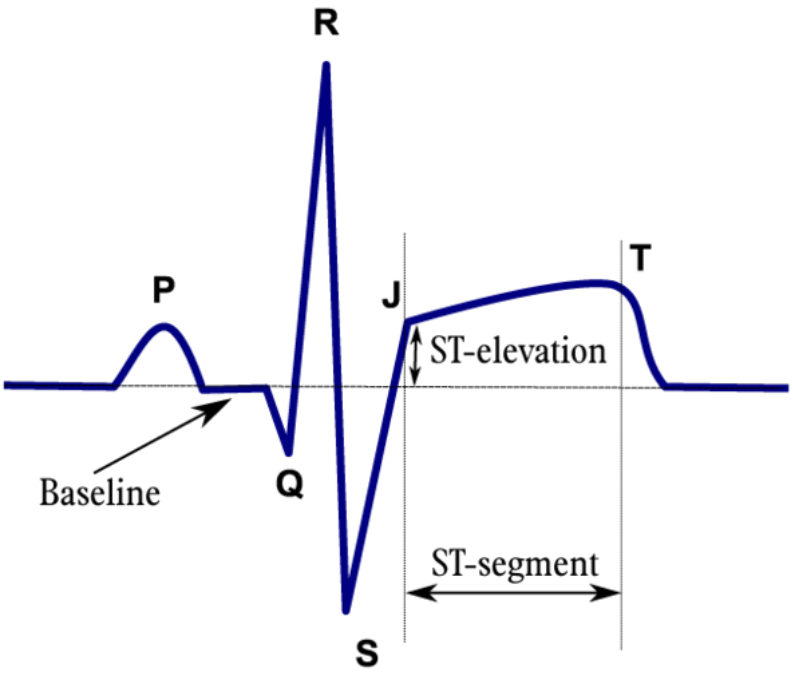

Figure 2. This schematic representation shows a typical ECG change in a myocardial infarction, including ST elevations, J point elevations, and pathologic Q waves.
(Source: Plus PNG EKG Images)

2.3.2 Heart pressure and volume changes

A proper pressure differential and adequate blood volumes between the four chambers of the heart, the pulmonary vasculature, and the systemic vasculature, are essential in maintaining proper heart filling and forward blood flow. These pressures and volumes are dynamic and vary depending on the stage of the heart cycle, but the changes will be consistent in a healthy heart. Therefore, abnormal changes in the pressures and volumes can be correlated to heart damage, and can be measured experimentally with the use of a pressure tracing catheter.

A pressure-volume loop (PV loop) is a physiologic diagram that is useful to visualize the pressure and volume changes in the left ventricle. By understanding the various pressure and volume changes in the heart, a researcher is able to better understand the significance of abnormal pressure and volume readings from an experimental catheter tracing, such as the readings performed in the Langendorff isolated heart model

The heart cycle begins with the closing of the aortic and pulmonary valves. This corresponds with the S2he second heart sound when auscultating the heart). During this stage, the left ventricle has ejected blood and the cardiomyocytes must now relax their contraction in order to allow blood to flow in once more. This is known as the “isometric relaxation” stage of the left ventricle (*figure 3*) and it is during this time that diastole occurs. As the left ventricle relaxes, the left atrium fills with oxygenated blood from the pulmonary veins and the atrium begins to contract. Once the pressure in the left atrium is greater than that of the left ventricle, the mitral valve will open allowing blood to fill the ventricle until the pressure in the ventricle becomes greater than the atrium, causing the closure of the mitral valve. The total volume that has entered the left ventricle is known as the “preload” and the pressure in the ventricle at this time is known as the “left ventricular end diastolic pressure (LVEDP)”. The closure of the mitral valve (the first

heart sound on auscultation) marks the end of diastole and the beginning of systole. The left ventricle begins to contract, but it is not able to overcome the pressure gradient initially that exists in the systemic vasculature, known as the "afterload", and so blood remains in the left ventricle until the afterload pressure is overcome in a stage known as "isovolumetric contraction". The aortic valve opens, and the ventricular ejection occurs, allowing the cycle to complete and the aortic valve to close to begin the cycle once more.

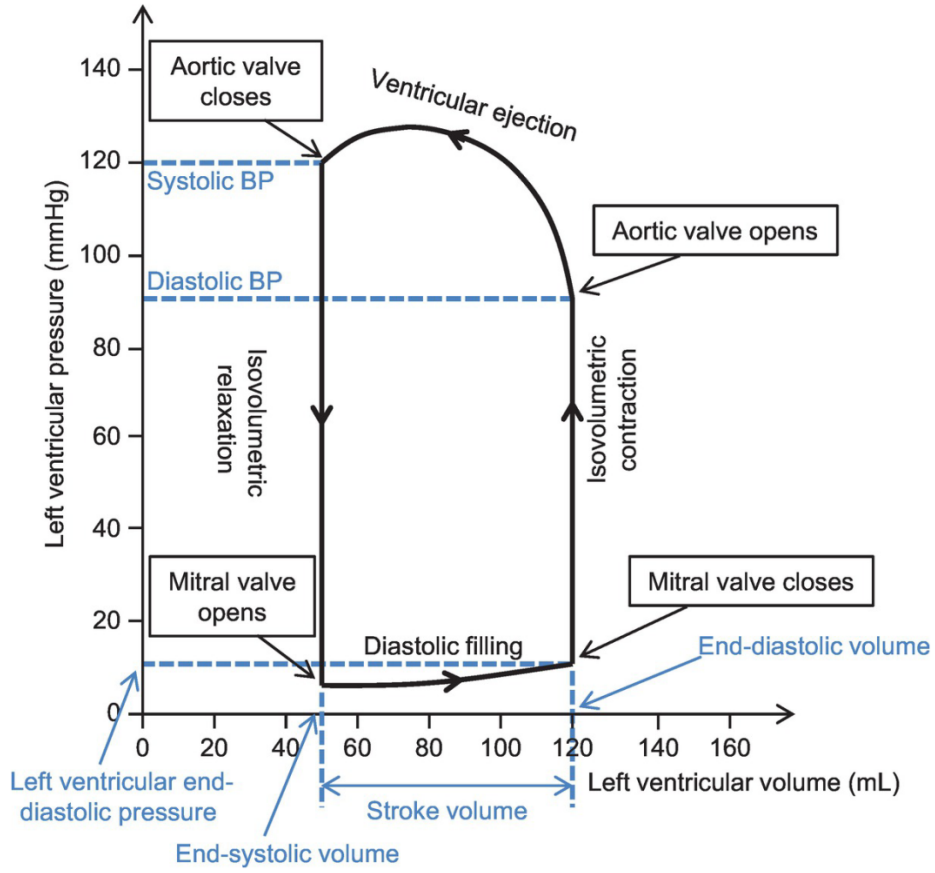

Figure 3. This schematic representation depicts the left ventricular pressure-volume loop. Arrows indicate opening and closing of the mitral and aortic valves. (Source: Plus PNG EKG Images)

Experimentally, obtaining pressures via a heart catheter, and understanding the PV-loop, allow the experimenter to obtain multiple pressure-volume parameters to give perspective on the physiologic function of the heart.

Stroke volume is defined as the volume of blood ejected during systole. It can be calculated by subtracting the left ventricular end diastolic volume (LVEDV) from the left ventricular end systolic volume (LVESV). Stroke volume is affected by changes in the cardiac preload, afterload, and contractility. For example, during exercise the body has increasing metabolic demands, and so more blood must be pumped to the systemic vasculature. In order to compensate for this, the heart will increase its contractility, heart rate, and venous return, allowing for a greater stroke volume to occur and meet the oxygen-demands of the tissues. MIR injury, adequate stroke volume often cannot be met due to the impaired function of the ventricle. This deficit may be due to arrhythmic changes, impaired relaxation due to calcium dysregulation, and the impairment of proper ventricular contraction [*Bruss et al., 2019]*.

The LVEDP is an important measurement of heart function, and represents the pressure in the left ventricle after it has received blood from the left atrium. In humans, this pressure ranges from 3 – 8 mmHg (Landsberg). In MIR injury, the left ventricle loses its ability to relax after contraction, and thus the chamber size of the ventricle is significantly decreased, causing abrupt increases in the LVEDP. Furthermore, MIR injury causes further ischemic damage, and the left ventricle loses its overall contractile ability. Due to this, the ventricle will not fully eject its preload, and a significant amount of volume will remain in the ventricle after systole, causing an increased LVEDP [*Mielniczuk et al., 2007]*. Therefore, observing an increase in LVEDP after ischemia is a reliable indicator of myocardial damage, and can be observed experimentally using a pressure-tracing catheter in the Langendorff model.

The LVESP is a measurement of the heart's pressure in the left ventricle after a full contraction. This pressure is influenced by multiple factors, such as the total preload, the total afterload, and the contractile ability of the heart. The LVESP may increase or decrease in heart injury, depending on the circumstance. For example, in chronic heart failure, the LVESP tends to increase due to increase fluid overload and poor heart contractility, however, in an acute myocardial infarct the LVESP may range from normal to decreased due to an impaired left ventricular preload.

The dP/dt max and min refer to the minimum and maximum rate of rise and fall in changes in the pressures of the ventricle. It is typically used as a measurement of ventricular performance, but it may vary depending on hemodynamic parameters such as blood flow or afterload. In MIR injury, an overall decrease in the dp/dt max and min may be observed due to the reduced contractile function of the ventricle. Measuring a final dP/dt max and min against a baseline reading after induced ischemia may be useful in determining the total amount of reduction in contractility of the heart.

Coronary flow is an important determinate of the overall oxygenation of the heart. Coronary flow happens during diastole, and in rats typically ranges from 10-15 ml/min depending on the oxygen demand of the heart. In MIR, the diastolic blood flow to the coronary arteries decreases due to a variety of reasons, such as eNOS dysregulation and increased calcium myocardial contractility, impairing the relaxation ability of the heart during diastole. Therefore, coronary flow is an important measurement in determining the overall damage to the myocardial tissues.

While one pressure or volume reading may not be adequate in determining the degree of cardiomyocyte damage in MIR injury, obtaining multiple different readings at multiple times may provide evidence of the overall picture in regards to MIR. The readings obtained

experimentally for our lab include the LVESP, LVEDP, dP/dT max/min, heart rate, coronary flow, and left ventricular diastolic pressure. These readings occurred every 5 minutes over the course of an entire experiment to create a picture of the overall physiologic changes in the heart after an MIR injury.

2.4 The clinical manifestations of MIR injury

The most obvious solution to an obstruction in blood flow to the heart is to re-introduce blood flow. This remains the standard of care clinically, but reperfusion after prolonged ischemia serves as a double-edged sword. While reperfusion will allow blood flow to return to ischemic tissue, cell damage is exacerbated by a cascade of biochemical events that result in further inevitable tissue damage. MIR injury can manifest as 4 different clinically relevant findings, including arrhythmias, myocardial stunning, microvascular obstruction, and lethal myocardial reperfusion injury.

Normal heart contraction and relaxation is essential for supplying adequate blood supply to the bodily tissues, as well as the heart itself. Due to the mitochondrial damage created by MIR injury, these normal physiological functions become compromised. Excessive calcium ions generated through the MIR pathway create excessive cardiomyocyte contraction. This excessive contraction prevents proper relaxation of the heart. Without proper heart relaxation during heart diastole, the filling capacity of the heart, or preload, becomes significantly reduced. In terms of cardiac parameters, MIR injury will increase the LVEDP due to increased cardiomyocyte contraction and impaired relaxation. Due to impaired relaxation, the total volume available in the left ventricular cavity, LVEDP, will decrease significantly. With reduced preload, the cardiac output of the heart will drop, and the amount of blood carrying oxygen that will be available to the coronary arteries, as well as oxygen demanding tissues distal to the heart, will become

impaired *[Klabunde, Cardiac Physiology]*. Other players affected in the MIR pathway, such as reduced Nitric Oxide generated by eNOS, may also play a role in impaired coronary artery flow due to reduced vasodilation *[Toda et al., 2011]*. Reduced cardiac output will have immediate effects on oxygen-demanding tissue, but downstream a low cardiac output also activates another pathway known as the Renin-Angiotensin-Aldosterone System (RAAS). A reduced forward systolic flow is sensed by the blood pressure-regulating cells of the kidney, known as the macula densa. The cells will respond by increasing the release of a potent hormone mediator of vasoconstriction called Renin. While Renin itself has intrinsic vasoconstrictive effects, it will also propagate further hormonal release of other potent vasoconstrictive hormones, such as Angiotensin II, Aldosterone, and Norepinephrine *[Fountain et al., 2019]*. These vasoconstrictors will increase the systemic blood pressure of the circulatory system, known as the afterload. An increased afterload will require the heart to contract harder against a larger pressure, demanding a larger oxygen supply and causing further ischemic damage. The cyclical and self-potentiating factors involved in MIR injury therefore become extensive, and the "snowball" effect of MIR injury becomes a devastating factor to those who suffer an MI. Decreased cardiac output will also be sensed by the pressure regulating cells in the carotid sinus and aortic arch, in a process known as the baroreceptor reflex. In response to a low flow state, the baroreceptors will increase activation of the sympathetic nervous system through a release of Norepinephrine and Epinephrine. These hormones have significant vasoconstrictive effects on peripheral tissues through activation of Alpha-1 receptors, but also will activate Beta-1 receptors on the heart, causing increased cardiac contractility and heart rate. The increased afterload through Alpha 1 agonism, as well as the increased contractility and heart rate will all increase the oxygen demand of the heart and cause further damage in a mechanism similar to the RAAS pathway. This

constellation of various pathways and cyclical cell death worsen clinical outcomes and may lead to eventual heart failure and death [*Armstrong et al., 2020]*.

It has been observed that reperfusion causing MIR injury also may cause life-threatening arrhythmias such as ventricular fibrillation. The dysregulation of MPTP's, as well as the dysregulation of the cardiomyocyte pH levels due to lactic acid build-up may play a role in MIR induced lethal arrhythmias *[Neri et al., 2007]*.

2.5 Current lab protocols

Current lab work focuses on myocardial ischemia reperfusion injury on a cellular, *in vivo* and *ex vivo* model. On a cellular level, the lab measures the effect of free radicals on isolated cardiomyocytes, and observes the effects of certain drugs on free radical injury, such as doxorubicin, and ways to reduce the free radical damage from them.

On an *ex vivo* level, the lab works on myocardial ischemia reperfusion injuries in isolated hearts and the effect of autophagy enhancers and reducers in cardiac function. These experiments are typically done via an isolated heart model, such as the Langendorff model.

The lab currently is establishing an *in vivo* model of MIR injury in mice by the left anterior descending artery occlusion model. By successfully establishing this model, the lab can introduce various experimental drugs in an effort to reduce the effects of MIR injury on the heart.

2.6 *Establishing a model*

Establishing a reliable, and reproducible model is not only essential, but may be one of the most difficult steps in an MIR study. There is currently a large arsenal of options available for studying MIR injury, from a molecular level to *ex vivo* models, and the appropriate study should

be used for measuring the factors that wish to be studied. For example, if a researcher wishes to obtain results on a molecular level, such as changes in concentrations of certain free radicals, then an isolated myocyte cell culture may be more appropriate, because it will allow the researcher to control the environment very precisely. However, if the researcher wishes to study results on a physiological level, such as changes in cardiac output or heart rate, then a model such as the *in vivo* LAD ligation, or Langendorff preparation, may be more appropriate. Animal models pose many difficult challenges that may be often overlooked. For example, accurately ligating the correct artery during each experiment is essential in producing accurate results, but is challenging due to the small size of the artery, and the user precision required to ligate the artery without causing damage to surrounding tissues. The goal of this study is to establish two experimental models for use in our lab that are reliable and will generate reproducible results. The first model is an *in vivo* Left Anterior Descending artery ligation model in mice. The second is an isolated heart model, called a Langendorff preparation, in rats. The two experimental designs are best for measuring physiological changes to the heart after MIR, such as heart rate, cardiac output, and percentage of infarction. These results can be confirmed by various methods, such as ECG findings, Evan's blue staining, and heart chamber volume changes.

2.6.1 LAD Model

The Left Anterior Descending artery provides essential blood flow for up to 70% of the cardiomyocytes of the human heart, and overall is the most commonly diseased artery in coronary artery disease. Surgically it is more accessible than other coronary arteries when accessing the heart via the anterior thorax due to its large size and anterior position on the heart [*Ogobuiro et al., 2020]*. Due to its clinical implication in heart disease, the LAD occlusion model has become a popularized animal study for simulating a myocardial infarction in humans.

In terms of the types of animals used, mice models have become increasingly popular. A study by Krishnan et al. concluded that the embryological cardiac development in mice and humans were similar, and the final anatomy of the two hearts had very few structural differences, making mouse hearts an excellent model for studying heart disease in humans. Furthermore, the expanding genetic engineering technology of mice, increasing availability of mouse-specific surgical tools and accessible costs make mice an ideal animal for MIR study models.

The LAD occlusion model has many strengths over other experiments used in MIR injury. Namely, it is beneficial in allowing to observe ischemic changes in a live animal, giving a more specific simulation of MIR injury compared to humans. An *in vivo* study may also benefit in reducing the amount of confounding factors that may affect *ex vivo* studies. For example, when removing the heart in the Langendorff model, the Renin-Angiotensin-Aldosterone system, as well as the Aortic baroreceptor response, in addition to many other systemic responses, no longer play a role. It is well known that these systems play a role in generating an overall clinical picture in cardiac disease [*Armstrong et al., 2020]*, and so allowing those processes to still occur in a live animal may represent a more clinically relevant study.

The LAD occlusion model requires precise surgical skills by the experimenter in order to properly yield results. Since the model is *in vivo*, the mouse must be continuously monitored for healthy vital signs. Furthermore, properly occluding the correct artery during each experiment, as well as performing proper surgical technique without injuring any vascular structures may be challenging. If the model is performed correctly, it provides a very accurate parallel of a natural MIR injury in humans and, thus, the results may be more representative of a human MIR injury.

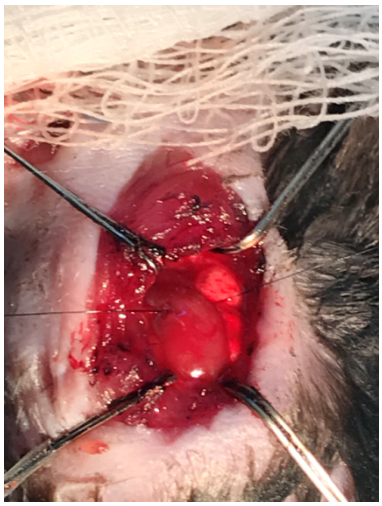

Figure 4. Identification of left anterior descending coronary artery in the mouse. This image demonstrates the exposed mouse heart in the LAD occlusion model. In this view, a Nylon suture was passed under the Left Anterior Descending artery.

2.6.2 Langendorff Model

The Langendorff Model was first established by Otto Langendorff, who performed an MI model through retrograde perfusion with a Krebs buffer. Today the model is widely used across many MIR studies due to its relative ease and ability to precisely control many physiological conditions.

Typically, a rat model is used, as the heart of the rat is large enough to be easily manipulated and hung up on the apparatus. The heart of the rat is excised under anesthesia, and the heart is hung from a staging model that will continuously perfuse a physiologic buffer. The buffer allows the heart to continuously pump on its own (a physiologic process called heart automaticity), which allows the experimenter to simulate a beating heart model. With the heart continuously beating, the experimenter can simulate an MIR injury by completely occluding buffer flow to the heart for a set amount of time, and then re-introducing the buffer. Throughout the experiment, various parameters can be studied with the use of a catheter, such as heart rate, ventricular volumes and pressures, and cardiac output. Various experimental drugs can also be used during the procedure to observe and effect compared to a control population. After the experiment has concluded, the experimenter is able to section and stain the heart to observe the overall infarct percentage.

A strength of the model is that its results are easily reproducible, and the procedure is generally easier for the user than the LAD ligation model. Since the animal has been euthanized,s and the only organ that requires monitoring is the heart, the model often has less random errors, compared to the LAD model where the mouse may suffer a variety of surgical complications resulting in injury or death that may compromise the data.

A disadvantage of the model is that it is *ex vivo*, and as such the results may not translate to clinical human research as well as an *in vivo* model would. For example, the isolated heart does not have an afterload that would represent the true peripheral vascular resistance in a living animal. Due to the fact that the heart is isolated, it is not a true working heart model, and such is subject to confounding factors that may not translate to human trials as well as a model such as the LAD occlusion model might.

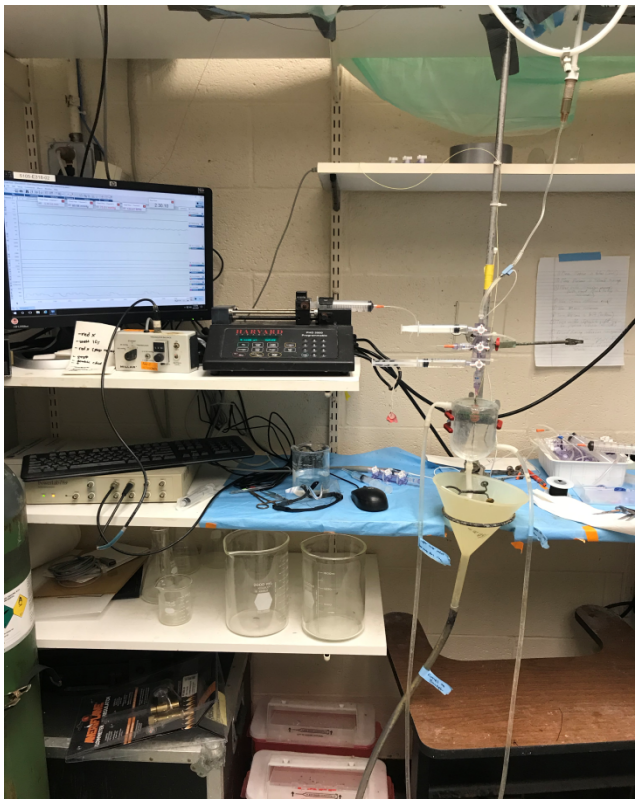

Figure 5. Langendorff perfusion of an isolated heart. This image depicts Langendorff perfusion of an isolated heart. This apparatus was used to conduct the *ex vivo* experiments. Hearts were isolated from euthanized mice and placed into the water-jacketed glass chamber containing Krebs buffer, a physiological solution,. The aorta was cannulated to provide retrograde perfusion of the heart with Krebs buffer in a temperature-controlled environment meant to simulate *in vivo* physiologic conditions.

III. Hypothesis

The hypothesis of the research is that ligation of LAD *in vivo* in mice hearts, followed by reperfusion, can induce MIR injury provable by ECG changes and by obtaining an area of total infarct in tissue stained hearts. In addition, MIR injury can be displayed by the Langendorff model, which will show changes in heart catheter readings and total area of infarct in tissue stained hearts. By establishing a reproducible model, our lab will be able to introduce various experimental operators, such as drug trials.

IV. METHODS

This animal protocol has been reviewed and approved by the Institutional Animal Care and Use Committee (IACUC). Mice (C57BL/6, 20-40 g, Charles River) were used for *in vivo* MI/R experiments. Mice (C57BL/6, 20-40 g) for LAD identification were donated by Dr. Bravo after euthanasia. Moreover, Sprague-Dawley rats (225-275 g, Charles River) were used for *ex vivo* MI/R experiments.

4.1 In vivo MI/R injury model

4.1.1 Identification of LAD by latex injection in sacrificed mice (Yoldas et al.)

1) **Anesthesia:** induct mouse using 2.5% isoflurane gas and 1 L/min oxygen.
2) **Preparation:** after ensuring proper anesthesia, euthanize mouse by means of abdominal aorta incision. Once euthanized, wash vessels of blood by injection 0.9% physiological saline into the aortic arch. Perform thoracotomy until visualization of the heart and its vessels is possible. In order to prevent leakage of dye, the super, inferior, and posterior vena cava must be ligated with a 6-0 suture.
3) **Injection**: inject latex dye into the aorta retrograde slowly until the coronary arteries can be visualized and contain the dye color.
4) **Polymerization:** remove the heart and submerge in normal saline solution at room temperature for an hour, allowing the dye to solidify in the heart.

4.1.2 In vivo MI/R injury model steps and protocol

1) **Anesthesia**: Mouse is initially inducted within a container ventilated with 2.5% isoflurane gas and 1 L/min oxygen for 5 minutes. To ensure induction, the mouse is monitored for slowed breathing rate.

2) **Preparation of mouse**: The mouse hair on the chest and neck is removed via applying *Nair* hair removal solution for 1-2 minutes until hair has been sufficiently removed and skin is clearly visible on chest and neck where surgery will commence. Proper induction of mouse can be monitored by observing breathing rate, monitoring pain response with tail compression, and observing heart rate from the ECG.
3) **Staging**: Stage is prepped by initially cleaning with an ethanol solution, then applying an electrode cream to each of the 4 limb leads on the stage. Tubing that contains isoflurane and oxygen is attached securely to the stage to allow placement of the snout of the mouse within (once transferred from the container to the stage). An ECG machine is turned on which will allow for monitoring of heart rate and ECG waveforms. The mouse is transferred to stage that is heated at 37.5 degrees Celsius, and placed in the supine position with each limb taped down on each of the 4 limb leads, while the snout of the mouse is placed within the breathing tube emitting isoflurane and oxygen.
4) **Intubation**: Intubation is set up via tracheostomy. First, the superficial skin over the area of the trachea is cut from inferior to superior, exposing the initial fatty layer as well as thyroid tissue and superficial muscles. With a blunt dissection tool, the fatty tissues are gently displaced until the trachea and its surrounding musculature are clearly visible. The muscle on the trachea is then gently dissected until there is a clear visualization of the trachea and its rings. Once a sufficient region of the trachea is visible, a 6-0 suture is placed under the trachea to allow for better control for the incision. The incision is made by pulling on the string to elevate the trachea, then cutting horizontally across the trachea until a sufficient sized hole is made. An intubation tube is immediately placed in the newly created tracheostomy hole, and connected to a ventilation machine. The ventilator

is set at a stroke volume of 250μL, and a respiratory rate of 150 breaths/min, with isoflurane at 2%.

5) **Surgery** - The left chest is dissected over the area of the heart, which can be localized with gentle palpation with a finger to feel for the heartbeat. A diagonal incision is made following the angle of the ribs. Once the skin has been dissected, the external chest muscles are dissected with a blunt forceps until the ribs are clearly visible. The third intercostal space is then dissected until there is a clear visualization of the heart within its pericardium. The pericardial layer can be removed by gently grasping it with a blunt dissector and pulling superiorly, allowing for full visibility of the heart and its vessels. The pericardium is pulled gently outwards to form a "tenting" around the heart, allowing the heart to be easier visualized. The left anterior descending (LAD) artery is then identified. Typically, the LAD is located towards the inferior and medial border of the left auricle. A dissecting microscope and two angles of light can aid in the visualization of the LAD. The LAD can also be better visualized by first locating the cardiac coronary vein, which often appears inferior to the LAD. Once visualized, a 7-0 nylon suture is passed through the heart under the LAD. Next, a small tubing is placed at the area of the desired occlusion, and then tied tightly with the nylon suture to begin the ischemic period. The ischemic period continues for 30 minutes, and ECG is monitored for changes. These changes should include an ST-segment elevation, T wave inversions, and/or pathologic Q waves. At the end of 30 minutes of ischemia period, the tubing is removed to introduce reperfusion. Pale bleaching of the heart can be observed and will further support proper ligation. The mouse heart is reperfused for 2 hours, with continued

monitoring of the ECG for data collection and to ensure survival throughout the entire surgery.

6) **Risk area and infarct area identification –** At the end of a 2-hour reperfusion period, the LAD is re-ligated and the heart is excised from the mouse. The heart is injected with 0.5% Evans Blue dye through the aorta retrograde to differentiate between risk area and non-risk area. The heart is frozen for 5 minutes in dry ice, then sectioned into 1mm slices and placed into a sectioned plate with 2% TTC enzyme solution to identify infarct area. The plate is placed in a warming bath at 37 degrees Celsius to allow for development of the stain of viable tissue for about 20 minutes. Finally, the plate is fixed with 10% formalin. The heart slices are then placed on a glass slide and imaged with a *Nikon* DSLR camera. Infarct areas will stain white without blue staining, viable areas at risk will stain red without blue staining, and the area not at risk will stain blue, as healthy tissue will easily take up Evan's blue while infarcted tissue will not.

   Groups: 12 mice total were used in the experiment. 7 were used in sham surgery with no artery ligation, and 5 were used in LAD ligation.

4.1.3 Parameters recorded in in vivo MI/R model

1. **ECG** - ECG recordings will be taken before ischemia, at 1 minute, 5 minutes, 10 minutes, 20 minutes and 30 minutes. Following ischemia, ECG findings will be taken at 1 minute of reperfusion, 3 minutes, 5 minutes, 10 minutes, 30 minutes, 60 minutes, 90 minutes, and 120 minutes. If a noticeable ECG change occurs but is not within the scheduled time frame, additional pictures will be taken of the event. Observing ECG changes will be vital in both accurately ligating the proper artery and monitoring the vitals of the mouse. At 1 minute of ischemia, hyperacute T-wave, or "peaked" T-waves

should be observed. These T waves are amplified higher than the baseline T-waves. ST-segment elevation should also be observed, and the ST-segment may remain higher throughout the entire ischemic period. Other ECG changes, such as a widened QT-interval and Q-wave deepening, will provide further evidence that the LAD has been properly ligated.

2. **Infarct percentage -** By taking high quality pictures of the Evans Blue + TTC stained heart, a percentage of infarct area, at risk area, and healthy tissue can be established and compared between models to determine if there is a significant difference of infarct size between groups. This is done by use of *Image J* software, which allows for accurate tracing of infarcted, at risk, and healthy tissue.

4.2 Ex vivo MI/R injury model in Isolated rat Heart by Langendorff preparation

4.2.1 *Ex vivo MI/R injury model steps and protocol:*

1) **Preparation**

1. Turn on the water bath (set to 42 °C) in order to heat the Krebs Buffer to the desired temperature range (e.g,, 37.4°).

2. Prepare 4.0L Krebs buffer (27.69g NaCl, 12.09g Dextrose, 1.74g KCl, 8.29g HCO_3, 3.95mL EDTA, 3.95mL $CaCl_2$, 3.95mL $MgCl_2$) and oxygenate.

3. Prepare anesthesia by placing rat in isolated chamber that is infused with oxygen and isoflurane. Typically, 2% isoflurane with 1L/min oxygen for 10 minutes is sufficient to induct anesthesia, but more time may be required depending on the rat. Sufficient anesthesia can be confirmed by pinching the tail of the rat and observing if there is a response.

4. Prepare a separate 50mL beaker with ice cold Kreb's buffer in order to transport the rat heart to the apparatus once excised.

5. Draw up 500U of Heparin in a 1mL syringe for injection into the mouse prior to heart excision.

2) Heart isolation

1. Anesthetize the animal using isoflurane and transfer the deeply anesthetized rat to the surgical stage area.

2. Inject rat with 1mL Heparin i.p.

3. Lift the skin of the abdomen with forceps and use scissors to make a horizontal incision across the abdomen inferior to the diaphragm.

4. Continue cutting the outline of the thoracic cavity towards the head of the rat, exposing the diaphragm. Gently cut the outline of the diaphragm, taking care not to cut any of the cardiac vasculature, and retract the ribcage superiorly from the xiphoid using forceps.

5. Apply gentle traction to the visible heart anteriorly to separate the heart from the other thoracic organs and place scissors posterior to the heart. Quickly excise the heart with scissors and transfer it to the ice cold Krebs buffer 50mL beaker for transport to the Langendorff apparatus.

3) Cannulation of the heart to the perfusion system

1. Transfer the heart to a flat dish and identify the aorta, which often can be seen by observing blood pumping through it. Gentle excision of other structures such

as the thymus and pericardial tissues may be necessary in order to properly visualize the aorta.

2. Once the aorta is visualized, grasp the walls of the aorta with two forceps and transfer it to the aortic cannula that should be dripping Krebs buffer.

3. Proper placement of the aorta is essential to properly perfusing the heart. The coronary arteries lie within the aorta about 1-2 mm superior to the aortic valve. Ensure that the cannula is not too deep or superficial by manually elevating or depressing the aortic root on the cannula.

4. Once the aorta is cannulated, apply forceps horizontally to hold the aorta in place, and pass a silk suture below the forceps. Tie the aorta into place by looping the silk suture twice around the aorta ensuring that it is sturdy and will not allow fluid to leak or the aorta to move on the cannula.

5. The heart should beat more rapidly once proper cannulation of the aorta is established. If the heart is not beating, adjustment of the aorta may be necessary until proper perfusion of the coronary arteries with the Krebs buffer begins.

4) Inserting pressure transducer to measure left ventricular pressures

1. Gently resect the pericardium and thymus tissues with scissors until the left atrium is clearly visible. Cut a small horizontal hole across the left atrium, large enough to allow the catheter to enter. Insert the pressure transducer into the left atrium and continue to push inferiorly until the catheter passes into the left ventricle. This can be confirmed by pressure traces within the normal pressure in the left ventricle.

5) Induction of Ischemia and reperfusion

1. Once the heart has reached a baseline heart rate and normal range pressure readings, induce ischemia by occluding the perfusion of Krebs buffer into the heart. Pressure tracings should immediately begin to fall and the heart rate will continuously drop until the heart is no longer beating.

2. Continue ischemia for 35 minutes, after which re-introduce Krebs buffer to the heart by re-opening the valve. A 10mL syringe filled with 5mL warm Krebs buffer was infused at the time of reperfusion at a rate of 1mL per minute, which serve as the MI/R control for future tested drug when it is administered in Krebs buffer at the beginning of reperfusion.

4.2.2 Data collection from ex vivo MI/R injury model

1) Heart rate, left ventricular pressure parameters (left ventricular end systolic pressure (LVESP), left ventricular end diastolic pressure (LVEDP), pressure over time (dp/dt) max and min), and coronary flow were recorded by taking continuous 10 second recording every 5 minutes at baseline (15min) and 45 minutes of reperfusion.

2) Infarction area detection and calculation: Once reperfusion has concluded, the heart was removed from the perfusion needle and place it into a heart sectioning device and place the device in a freezer. The heart is frozen for 30 minutes, then sectioned into 1mm slices and placed into a sectioned plate with 2% TTC enzyme solution. The plate is placed in a warming bath at 37 degrees Celsius to allow for development of the stain for about 10 minutes. Finally, the plate is fixed with 10% formalin. The heart slices are then placed on a glass slide and imaged with a *Nikon* DSLR camera.

3) Infarct percentage is acquired in two ways. First, using Image J to outline ischemic tissue and healthy tissue, and obtaining a total percentage of infarcted tissue. Second, by manually cutting the infarcted tissue and weighing it, then obtaining the total weight of the heart and dividing the infarcted weight by the total weight to obtain a total infarct percentage.

4.3 Data analysis and statistics

All data in the following text and figures are presented as mean ± standard error. Statistics were analyzed by student t-test. Probability values of $p<0.05$ are considered statistically significant

V. Results

5.1. In vivo MI/R injury model

5.1.1 Identification of LAD by latex

Proper identification of the LAD is essential for establishing regional MIR injury that involves ligation of the LAD. In a live mouse, the rapid heart rate and faint pink color of the LAD make identifying the artery challenging. By understanding the anatomy of the mouse heart, and by using landmarks such as the left auricle and cardiac vein, the experimenter is able to approximate the location of the LAD more easily.

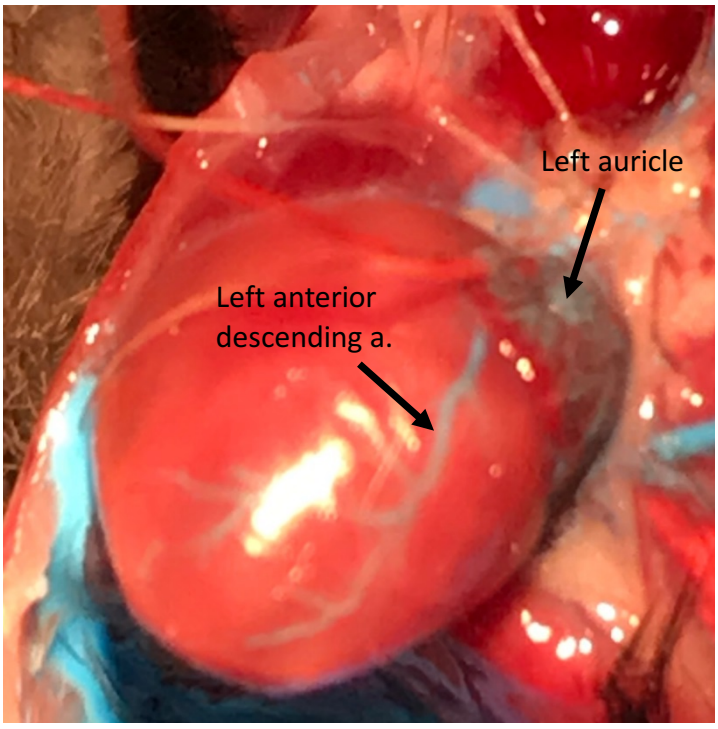

Figure 6. Latex dye staining of mouse heart. The left anterior descending artery (LAD; arrow) is seen in a mouse heart following retrograde injection of blue latex into the aorta. These injections enabled much easier identification of the LAD.

Figure 6 is a result from the experiment showing a mouse heart from an anterior viewpoint. The left anterior descending artery was labeled and clearly visible in blue. The origin of the LAD was the aortic root, however, it was often covered by the left auricle as seen. The LAD appeared inferior to the left auricle about midway if measured vertically. The LAD progressed towards the apex of the heart with multiple small branches trailing from it. By having a strong idea of the origin, surgically ligating the LAD becomes much easier during an *in vivo* experiment.

5.1.2 ECG changes during MI/R

Baseline and infarct ECG changes in mice were very similar to ischemic ECG changes in humans. At baseline, the atrial depolarization was represented by the "P" wave, ventricular depolarization was represented by the "QRS" complex, and ventricular repolarization was represented by the "T" wave (Baseline ECG can be seen in figure 7). Positive ischemic changes could be confirmed by observing various ECG changes, including T wave inversions, J-point rises and ST-segment elevations (example ischemic ECG changes can be seen in figure 8).

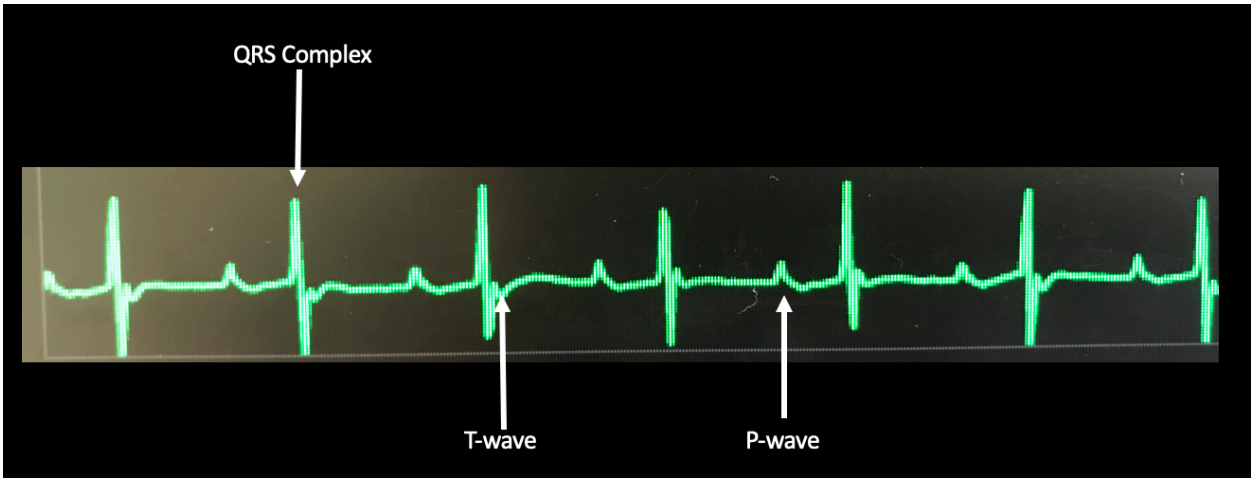

Figure 7. Normal Mouse ECG tracing. This imageshows a baseline ECG in mice with a normal QRS complex, T wave, and P wave as indicted by arrows.

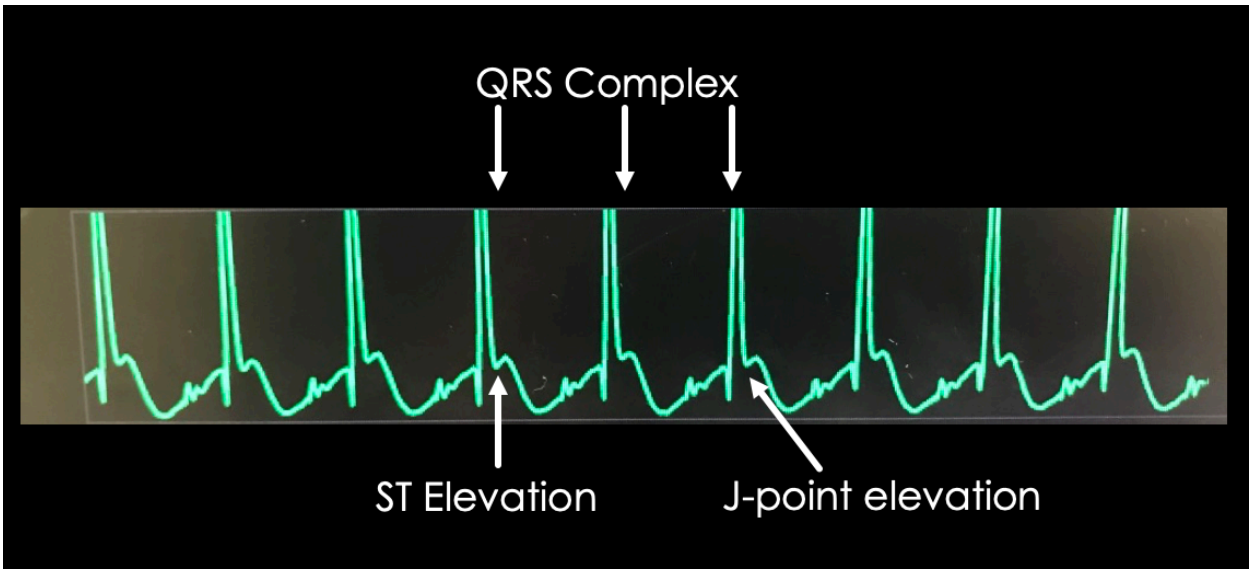

Figure 8. ECG Tracing of Ischemic Mouse Heart. The image shows a typical ECG in an ischemic mouse, with diffuse ST-segment elevation as well as J point changes as indicated by arrows.

A successful experiment began by first establishing a baseline ECG, and observing changes beginning from ischemia. Typically, T-wave changes were the first ECG abnormality to occur, and in most cases occurred immediately after ligation of the LAD. Figure 9 and 10 show a successful ligation, beginning with a normal baseline ECG to the end of reperfusion. At the time of ischemia, immediate changes in the QRS complex were observed including QRS widening an increase of the amplitude of the complex. T wave changes were seen with a more profound T wave change beginning at two minutes into ischemia. ST-segment elevations and J point changes began to occur as soon as 5 minutes ischemia, and gradually raised throughout ischemia.

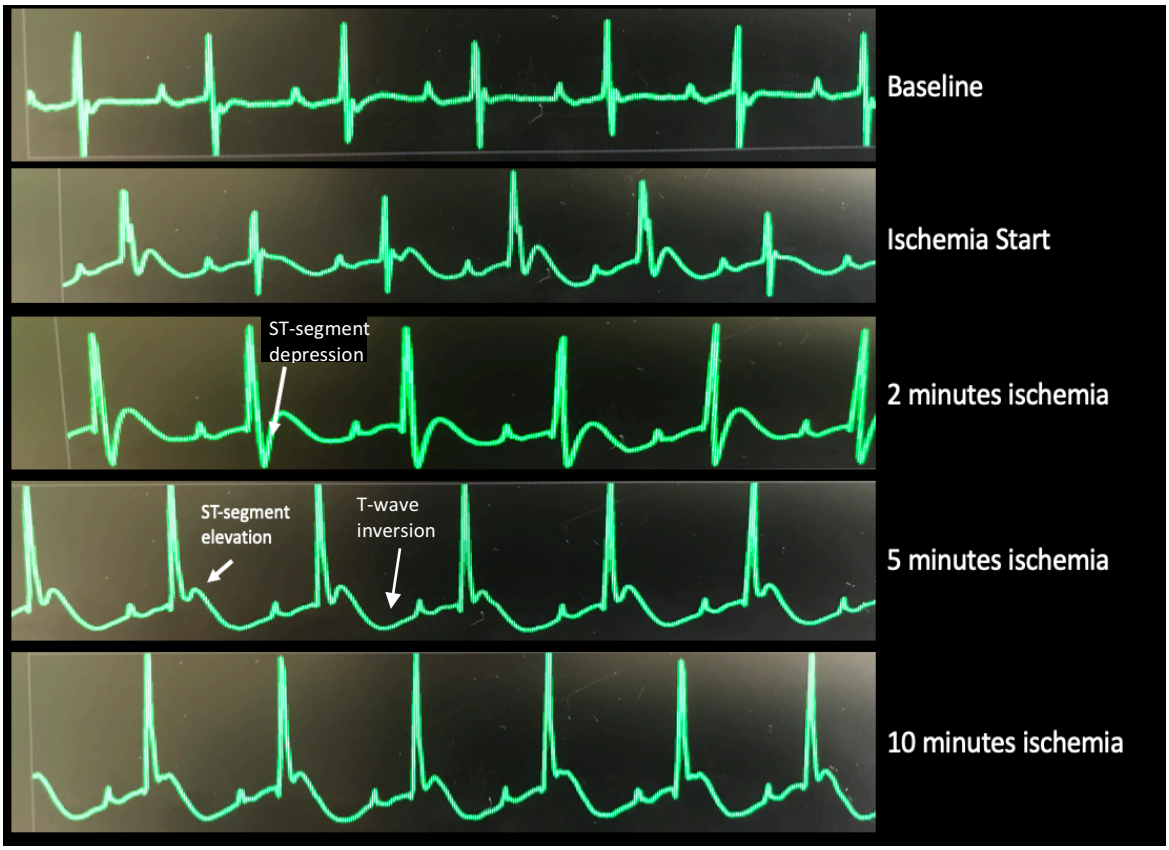

Figure 9. ECG Tracing of Mouse Heart with LAD Ligation. The image reflects the changes in the ECG tracing of an LAD-ligated mouse heart showing ECG changes from baseline to ten minutes of ischemia.

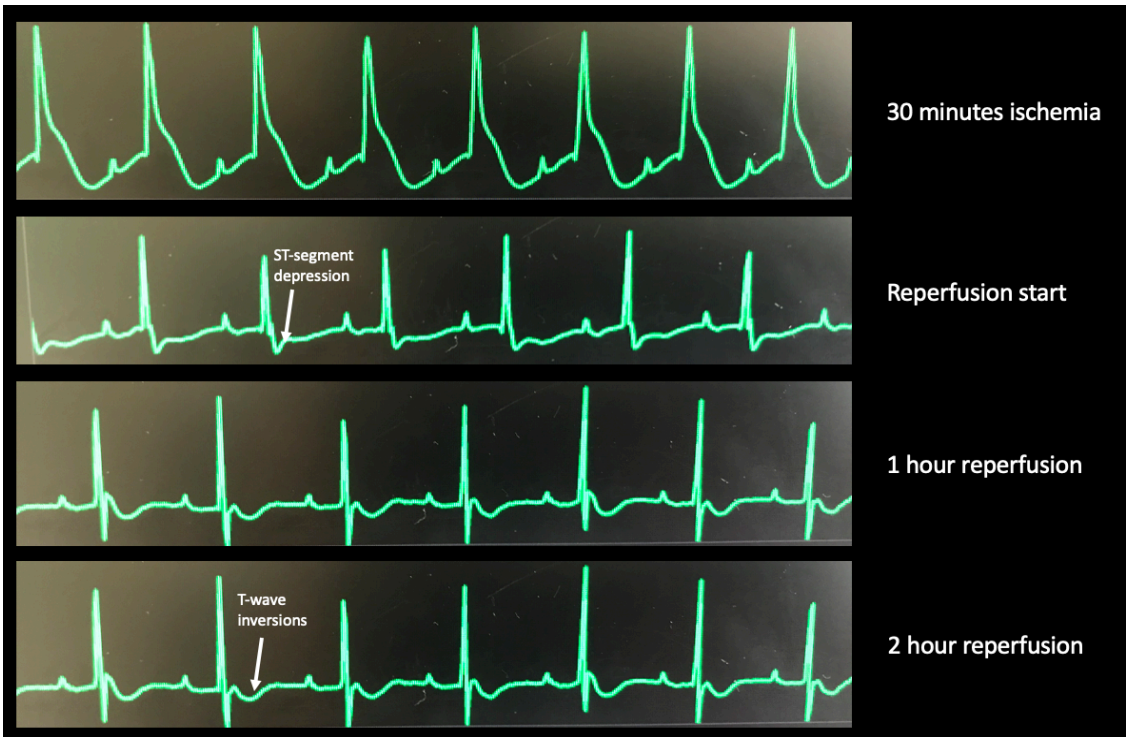

Figure 10. ECG Tracing of Mouse Heart After LAD Ligation. The image reflects the changes in the ECG tracing of an LAD-ligated mouse heart showing immediate changes after reperfusion, including ST-segment depression and T-wave inversions.

5.2 Factors related to the successful establishment of myocardial ischemia and reperfusion

5.2.1 Suture needle size

Proper suture size is essential in ligating the LAD. We found that a large suture, such as a 6-0 nylon, caused too much damage to the fragile mouse heart during ligation. Often, the heart would bleed excessively from the large puncture wound of the 6-0 suture. On the contrary, we found that the 8-0 suture was too thin, and although there was little bleeding, adequate pressure on the LAD could not be established due to the thin suture effectively cutting through the tissue and becoming loose. We found the best suture for ligation was a 7-0 suture.

5.2.2 Identification of LAD

Proper identification of the LAD is challenging considering the rapid heartbeat and the color of the artery, which blends in with the heart tissue. Furthermore, the cardiac veins often can be confused with the artery , but often the veins will be darker than the arteries. The latex injection model shown in Figure 1 was useful in determining the normal anatomical location of the LAD, which typically arose from the medial auricle and continues down the anterior surface of the heart towards the apex. The use of the cardiac vein may also aid in identification of the LA.D Typically the LAD is superior and slightly medial to the cardiac vein, which travels from the left lateral surface of the heart horizontally and meets perpendicular to the LAD. Applying gentle pressure with a small cotton tip often was helpful in identifying the LAD. By applying pressure at the proper location, the cardiac tissue should turn pale at the tissue inferior to the pressured spot. Finally, using a dissection microscope and two light sources from different angles helps to differentiate the various veins and arteries in the heart.

5.2.3 Sustained ligation

Sustaining ligation is challenging due to the tendency of the suture to loosen from the rapid heartbeat of the mouse. By using a small piece of plastic tubing, and by tying two tight surgical knots, adequate pressure can be insured. Often, the experimenter had to recheck the ligation and re-secure the suture to ensure that the artery is properly occluded.

5.2.4 Ischemia/Reperfusion induced arrhythmias

Arrhythmias are a common result of extensive myocardial damage from MIR injury, and often times were observed during the experiment at various times of reperfusion. The most commonly

witnessed arrhythmias were ventricular tachycardia, ventricular fibrillation, and heart block, which often resulted in the demise of the mouse.

5.3 Evans blue/TTC Staining Results

Successful stain with TTC and Evan's Blue dye show a clear contrast between healthy tissue (blue), an area of tissue at risk (pink/red), and the infarcted area (white). These can be seen in Figure 11.

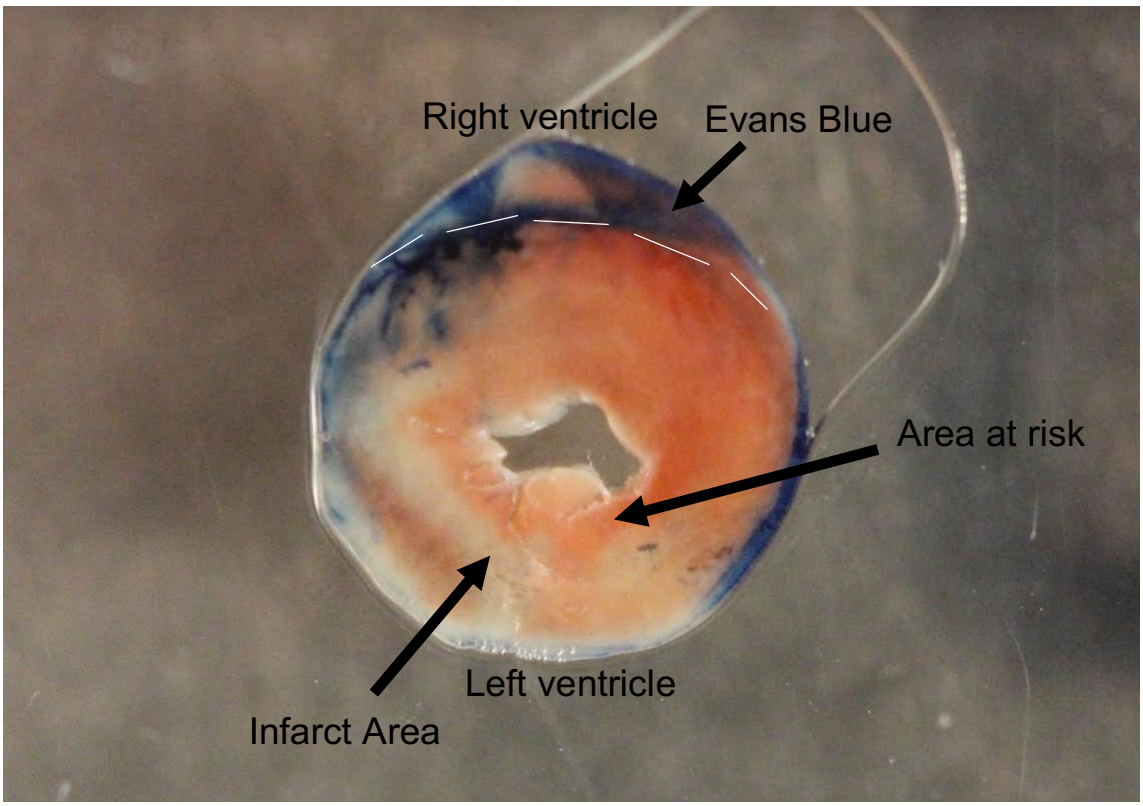

Figure 11. Evans Blue Dye and TTC Staining of Ischemia in an LAD-Ligated Mouse Heart. This image shows a clear color contrast between ischemic tissue (white,) tissue at risk (pink/red,) and healthy tissue (blue) in a mouse heart following LAD ligation and staining with Evans Blue dye and TTC.

In the above result, successful delineation between areas is visible. The healthy tissue, stained in Evan's Blue, is visible primarily in the right ventricle. This result is appropriate with the ligation of the LAD, because the right ventricle primarily receives its blood supply from the right coronary artery and its branches, and therefore should not be damaged. The area at risk can be seen as red/pink tissue, and infarcted tissue can be seen as white tissue on the anterior surface of the heart.

5.3.1 Factors related to successful Evans blue/TTC staining

Proper TTC staining is essential for identifiable delineation of the tissues. The technique was altered multiple times and expanded upon in order to successfully complete the experiments. The TTC solution used was changed in order to determine whether tissue staining was better with a different brand, and was found to be better after changing brands. The concentration of TTC was also adjusted from 1% to 2%, which gave better staining. The heart was initially frozen in a freezer, but we found that flash freezing of the heart on dry ice allowed for less time for ischemic change to occur after extraction from the mouse. Duration of time in the water bath also affected the final stain of the tissue. Leaving the TTC stained hearts in warm water for too long would often cause the stain to become light, and harder to distinguish the infarct tissue from at risk tissue.

5.4. Ex vivo MI/R injury model

5.4.1 Influence of Ischemia time on cardiac parameter after MI/R

Catheter reading changes are done to record the changes of the physiologic parameters of the heart. A difference between an initial versus end point reading signifies that damage to the heart has occurred, and by observing similar changes across multiple experiments, indicates that the

experiment is reproducible. Four rat hearts in total were used for these experiments. The LAD was occluded for 35 minutes, and the heart was reperfused for 45 minutes. Various parameters were measured during the experiment, and their means and standard deviations were calculated.

5.4.2 LVESP and LVEDP

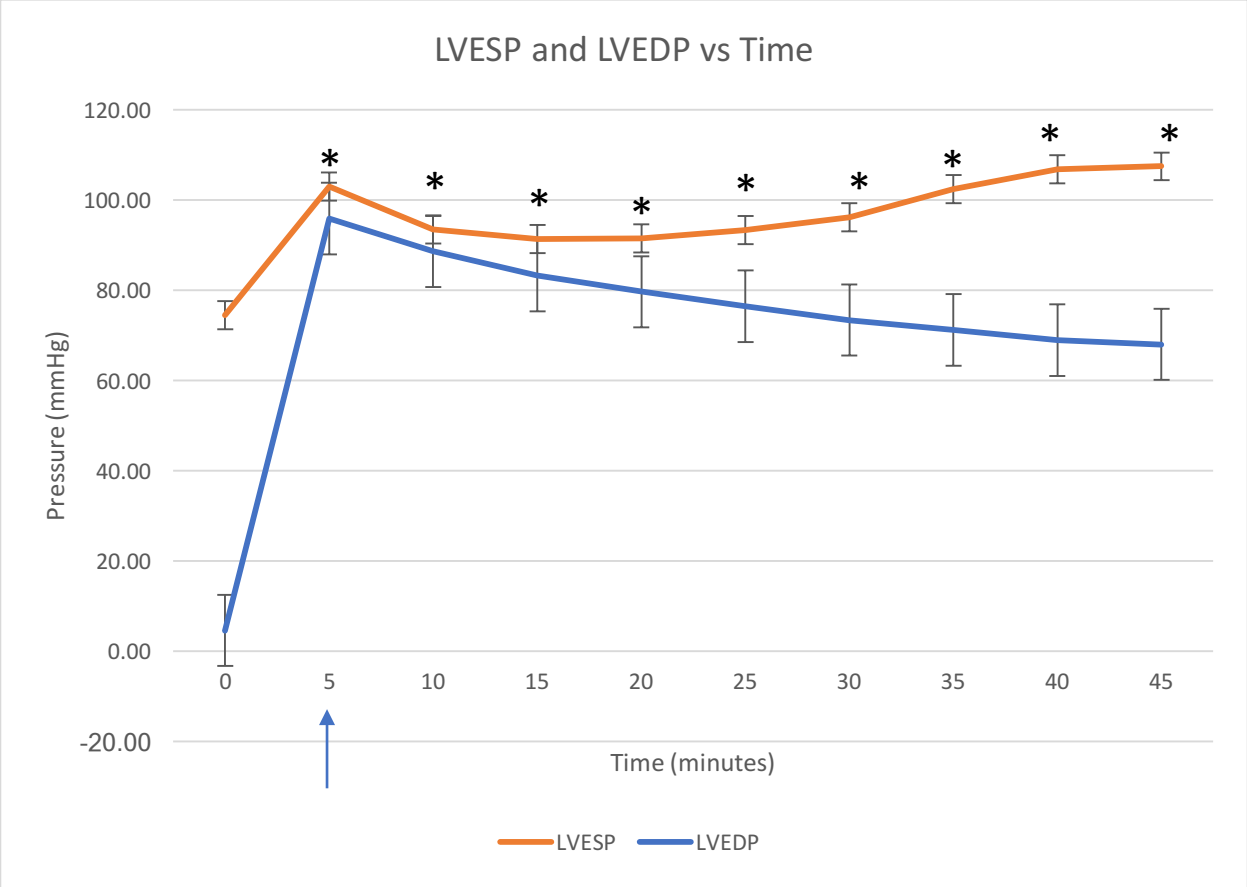

Figure 12. Changes in LVEDP and LVESP with Time. The graph reflects the time course of ischemic changes in LVEDP and LVESP in the mouse heart caused by LAD ligation. An arrow indicates the onset of reperfusion. *Asterisk (*) indicates significant difference when compared to sham control.*

Time course of LVESP and LVEDP (n=4) is shown in figure 12. During reperfusion, the LVESP showed a increased value at 5 minutes (102.91 ± 9.91mmHg, $p<.03$) compared to baseline (74.40 ± 2.77mmHg). Thereafter, LVESP had slightly reduction between 5-30 min, then slightly increased to 107.42 ± 3.82 mmHg $p<.05$ at end of 45 min reperfusion.).

LVEDP was low at the baseline (4.55 ± 0.26 mmHg). During reperfusion, it increased to 95.86 ± 9.66 mmHg at the 5 min. Thereafter, LVEDP gradually decreases throughout reperfusion until 45 minutes (67.95 ± 3.16 mmHg).

5.4.3 dP/dT max

The time course of dP/dT max between sham (n=5) and IR (n=4) hearts are illustrated in Figure 13. Initial dP/dT max baseline before ischemia were similar between MIR and sham control groups. There were no significant changes in the sham hearts. By contrast, MIR group showed significant reduction of dP/dT max starting from 5 to the end of 45 minutes when compared to sham hearts ($p<0.05$). At 5 min reperfusion, the dP/dT max were 130.08 ± 28.73 mmHg/sec and 1823.93 ± 374.34 mmHg/sec for sham and I/R hearts, respectively. At 45 min reperfusion, the dP/dT max were 779.37 ± 102.90 mmHg/sec and 2021.62 ± 273.20 mmHg/sec for sham and I/R hearts, respectively.

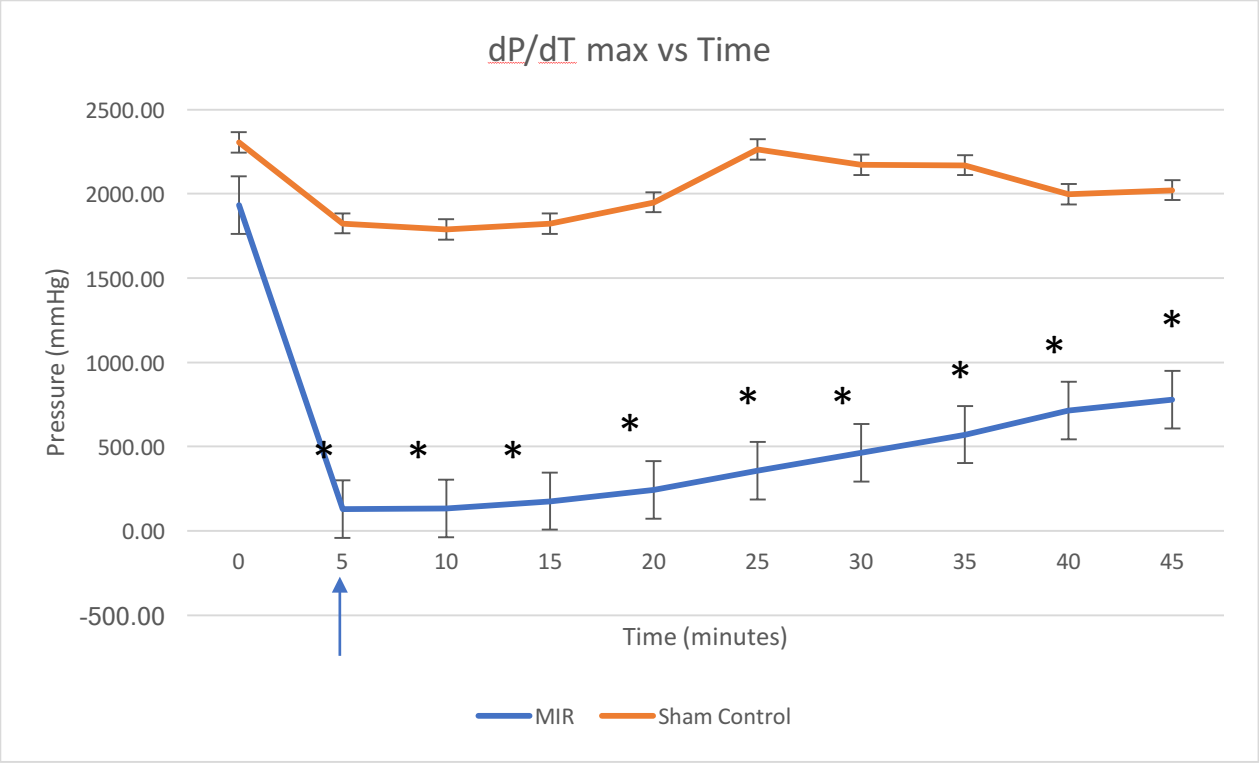

dP/Dt+ = max rate of rise of contraction in left ventricle during isometric contraction

*p<0.05 vs baseline

Figure 13. Changes in dP/dt max with Time. The graph reflects the time course of ischemic changes in dP/dT max in the mouse heart following LAD ligations. An arrow indicates the onset of reperfusion. Asterisk (*) indicates significant difference when compared to sham control.

5.4.4 dP/dT min

Initial dP/dT min between MIR and sham control groups were similar (Figure 14). By contrast, MIR group showed significant increase compared to sham control group at every 5-minute interval up to 45 minutes ($p<0.05$). The MIR group showed a significant increase in dP/dT min at 5 minutes (-105.39 ± 17.46 mmHg/sec) compared to sham control (-1134.19 ± 378.96mmHg/sec). dP/dT min values in the MIR group remain increased throughout reperfusion

but slowly decrease until 45 minutes (-627.20 ± 169.08mmHg/sec), while sham control remains unchanged at 45 minutes (-1475.38 ± 189.74mmHg/sec).

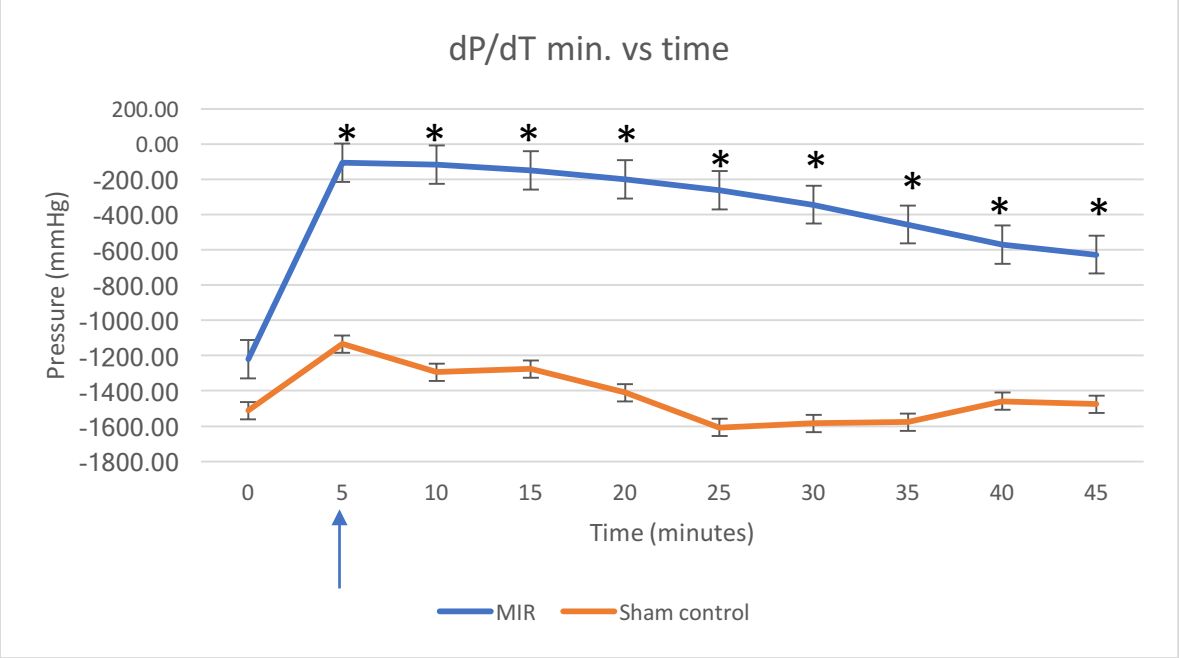

Figure 14. Changes in dP/dT min versus Time. The graph reflects the time course of ischemic changes in dP/dT min in the mouse heart caused by LAD ligation. An arrow indicates the onset of reperfusion. *Asterisk (*) indicates significant difference when compared to sham control.*

5.4.5 Heart Rate

Heart rate between MIR and sham control groups show no significant difference at any time during the course of the experiment. Initial heart rate of the MIR group (263.40 ± 6.5 bpm) and the control MIR group (261.91 ± 6.30 bpm) remained similar at all time courses until 45 minutes in MIR (259.70 ± 20.16 bpm) and sham control (267.38 ± 9.63 bpm). There was no significant difference in heart rate in the MIR group compared to the sham control group.

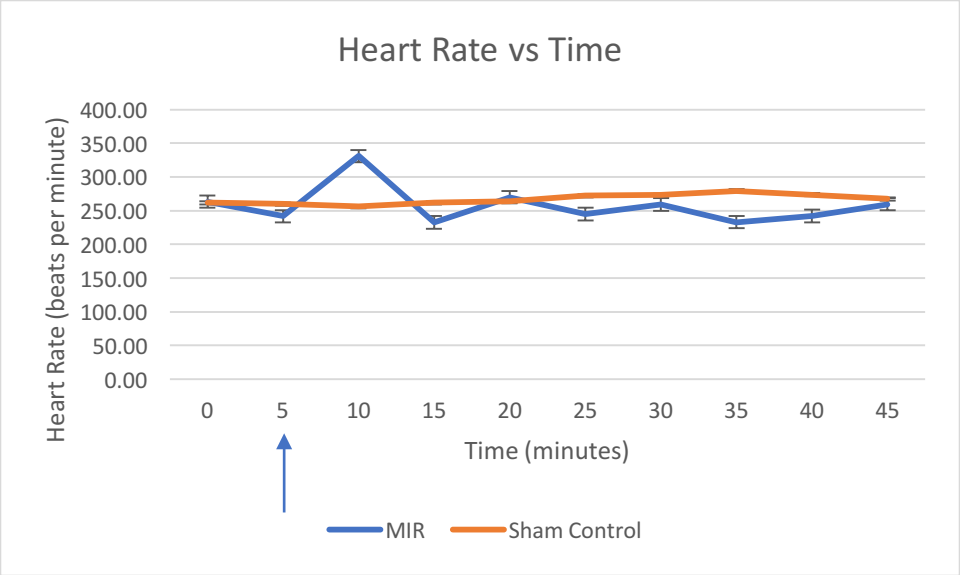

Figure 15. Changes in Heart Rate versus Time. The graph reflects the ischemia-induced time course of changes in heart rate in the mouse heart following LAD ligations. An arrow indicates the onset of reperfusion. No significant changes in heart rate were noted with myocardial ischemia.

5.4.6 Coronary Flow

The time course of coronary flow in MIR and Sham Control groups are reflected in Figure 16. The initial coronary flow baseline before ischemia between MIR and sham control were similar. After reperfusion, the MIR group showed a significant decrease in the coronary flow compared to sham control ($p<0.05$). The MIR group shows a dramatic decrease in coronary flow at 5 minutes (1.97 ± 1.16 ml/min) compared to sham control (15.40 ± 3.41 ml/min). Coronary flow in the MIR group slowly increased throughout reperfusion but never returns to its initial value, compared to sham control which remained relatively unchanged. The final coronary flow of the MIR group was 7.75 ± 2.43ml/min, compared to sham control at 17.06 ± 2.43ml/min.

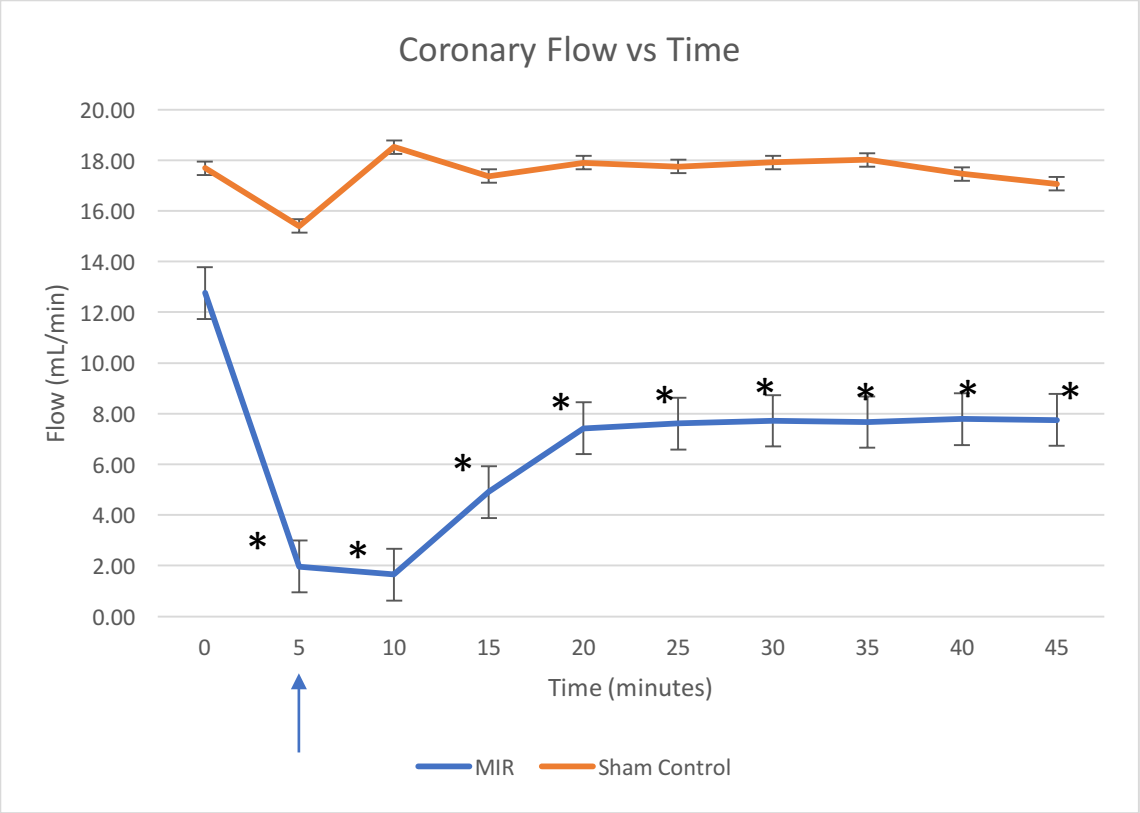

Figure 16. Changes in Coronary Flow versus Time. The graph reflects the time course of ischemic changes in coronary blood flow in the mouse heart caused by LAD ligation. An arrow indicates the onset of reperfusion. *Asterisk (*) indicates significant difference when compared to sham control.*

5.4.7 Infarction percentage in ex vivo MI/R injury

Representative pictures of infarct size in the MIR group were shown in Figure 17 The MIR group showed a relatively large white ring of dead cardiomyocytes on the edge of the cross sectional slice.

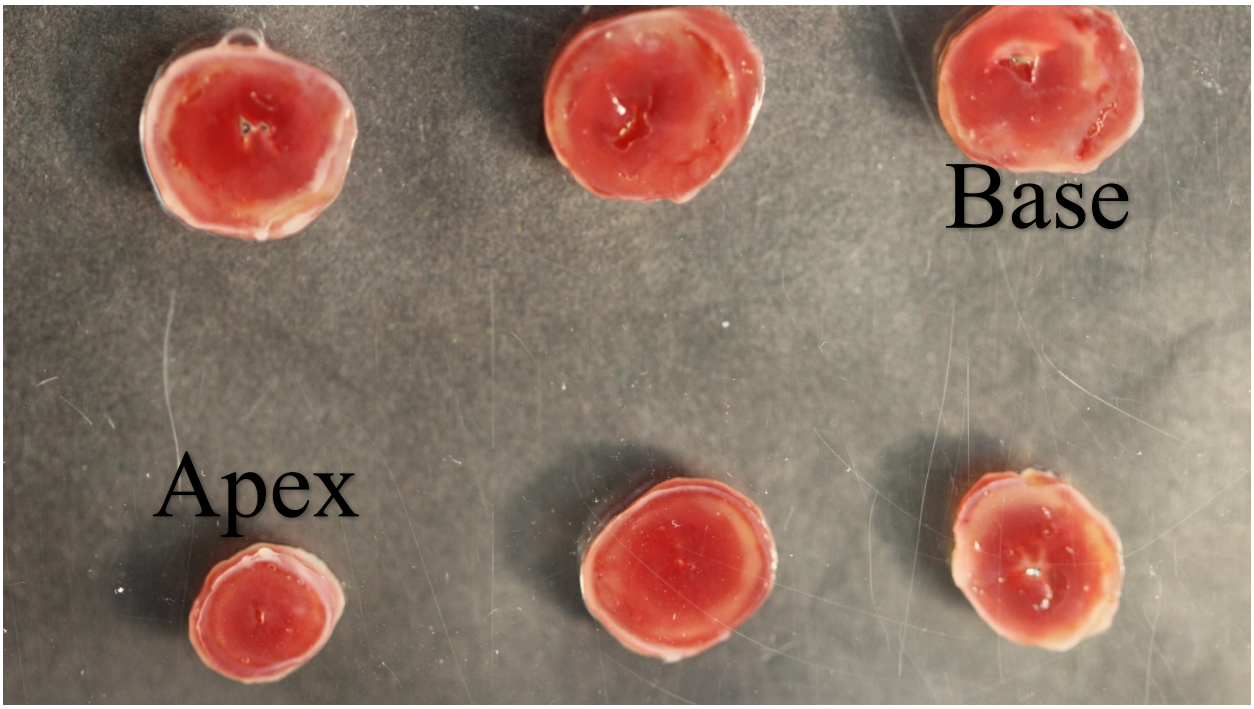

Figure 17: Image of sectioned rat heart after Langendorff experiment.

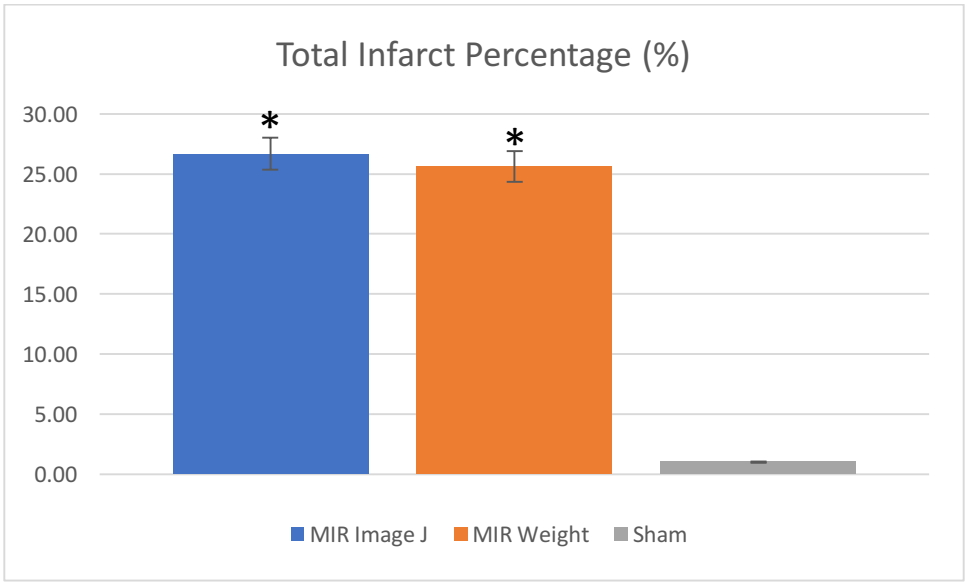

Figure 18. Total Infarct Percentage between MIR Image J, MIR Weight and Sham groups.

Asterisk (*) indicates significant difference when compared to sham.

The summarized infarction percentage between MIR and sham is shown in Figure 18. For MIR heart, Infarct percentage in Image J analyzed tissue was 26.68±1.89 %, while infarct percentage in weight analyzed tissue was 25.60±1.21%, which was similar as Image J measurement. By contrast, the total infarct percentage was less than 1% in the sham hearts.

VI. Discussion

6.1 Summary of Findings

The results of this study show that MIR compromises cardiac function in both the isolated heart model and the LAD occlusion model as can be seen by a significant change in the ECG, a significant increase in LVEDP, an increase in LVESP, decrease rate of pressure changes (ex: dP/dT max and min), decreased coronary flow, and a large infarct size when stained with TTC.

6.2 Electrical abnormality during MIR: ECG changes

An ECG is a valuable tool in assessing cardiomyocyte damage, as well as assessing whether coronary blood flow has been restored after reperfusion. In our study, we found that ST-segment elevations, and elevations of the J point after induction of ischemia, while successful reperfusion will result in a rapid decrease in ST elevations due to the normalization of cellular potentials in the ischemic tissue.

When the heart is in an ischemic state, several changes occur on an electrophysiological level that ultimately result in changes that are visible on an ECG. Hypoxic conditions will eventually lead to a loss of intracellular concentrations of ATP. This loss of ATP causes the failure of several ATP-dependent transport systems, notably the Na^+/K^+-ATPase that maintains physiologic levels of Na^+ and K^+ concentrations in the cellular space. Normally, this pump extrudes Na^+ out of the cell and pumps K^+ into the cell. However, when the function is lost, the extracellular concentration of K^+ increases. Futhermore, K_{ATP} channels, which also aid in maintaining physiologic levels of K^+, are compromised. [*Pharmacol et al., 2009])* The large extracellular concentration of K^+ changes the resting potential of the myocytes, ultimately causing a number of changes to the cell environment, such as increased depolarization, shortened

action potentials, and decreased conduction velocity. Together, these culminate in a number of waveform abnormalities that are visible on an ECG.

ST segment changes are typically one of the first visible changes that occur on an ECG during cardiac ischemia. ST segment elevation occurs when the ventricle is at rest and repolarized. Ischemic tissue will depolarize due to the improper handling of K^+ ions, and the depolarized ischemic tissue will generate an action potential that is recorded by the ECG as traveling away from the electrode. [*Hausenloy et al., 2020]* The generation of a depolarization during the repolarization stage of the ventricle will actually shift the baseline voltage that is recorded by the ECG to a more depressed state. When the healthy cardiomyocytes do eventually depolarize, zero voltage is recorded by the electrode, causing a negative ECG recording in the resting state. The net effect of the decreased baseline voltage, in combination with depolarization from ischemic tissue is an ST segment that appears elevated. The presence of an ST segment elevation typically correlates with a more severe infarction such as a transmural infarction, while ST segment depressions may be more common in subendocardial infarctions. The size of an ST segment elevation may also correlate with the amount of ischemic damage that has occurred, however, a baseline ECG has many variances. In humans, a myocardial infarction is only diagnostic by ECG if the elevation is at least greater than 1mm. The reintroduction of blood-flow to ischemic tissues, and thus ATP, will allow the Na^+/K^+-ATPase to return to function, as long as the cells are not permanently damaged. This will allow cardiomyocytes to properly sequester potassium ions back into the cells, reducing the action potentials generated by ischemic tissue and decreasing the ST-segment elevation [*Klabunde]*. However, if the ischemic duration is long enough to cause permanent damage, in combination with the effects of MIR injury, then there may be permanent changes to the ECG.

One change that may remain prominent on an ECG after an ischemic event and MIR injury is the presence of T wave abnormalities. T waves normally represent the repolarization of the ventricle after the QRS complex. The T wave is unique because it presents as a positive inflection on an ECG, even though it is a repolarization event. This is because the last ventricular cells to depolarize are subepicardial cells. These cells repolarize faster than the cells in the subendocardium, and this repolarization travels away from the electrode, causing a positive voltage appearance on the ECG [*Amanakis et al., 2019]*. The distinction in the type of cell damaged is important in the context of ischemia. If the subendocardial tissues are damaged in an ischemic event, they will begin to depolarize and repolarize more quickly than the subepicardial cells. The large repolarization by subendocardial cells is recorded as traveling towards the electrode (rather than away as it normally is) and will instead appear as a T wave depression. Typically these subendocardial cells are more susceptible to ischemia, and thus T waves can remain present even after reperfusion.

Another common waveform that may occur after ischemia is a Q-wave. The Q-wave occurs as a negative deflection in the ECG just prior to the QRS complex. Q-waves are typically evidence of a prior ischemic event, and usually do not appear immediately after an infarction. While T wave inversions and ST segment elevations are due to improper depolarization, Q-waves are due to the absence of depolarization from cardiomyocytes that have died. Q-waves will usually persist indefinitely [*Cardiovascular Physiology*]. Our experiment did not observe Q-waves, most likely because the heart was not reperfused for a long enough time for the dead tissue to become completely electrically inactive. In humans, Q-waves typically do not appear until 2-3 days after reperfusion.

Pressure Changes

6.3.1 LVESP/LVEDP

LVESP is a measure of the pressure inside the left ventricle after contraction. In rats, a healthy LVESP ranges from 70-80 mmHg. An increase in LVESP after cardiac injury can be due to both an increase in fluid in the left ventricle due to incomplete contraction, and due to increased working pressure required of the heart due to infarcted tissue.

LVEDP is an important physiologic measurement of heart function. Typically, a low LVEDP equates to successful ejection of the cardiac preload and proper filling of the ventricle during diastole. An increase in LVEDP equates to an inability for the heart to successfully propel blood forward in the left ventricle to the systemic circulation, causing retrograde flow of blood within the ventricular cavity that accumulates during diastole [*Cardiovascular Physiology]*.

The reduced cardiac function from MIR injury is primarily caused by cellular disturbances. During ischemia, ATP production will decrease due to the lack of oxygen, causing the cardiomyocytes to favor anaerobic respiration. This increase in anaerobic respiration will increase the acidity of the cells, due to an increase in lactic acid generation, and will impair the pH balance of the cells and, thus, it will disrupt cell homeostasis. During reperfusion, free radical generation occurs from multiple sources, notably the mitochondria. Normally, the mitochondria produces ATP by generating an electrochemical gradient in the electron transport chain in order to produce a driving force for ATP Synthase. In the presence of an MIR injury, the mitochondria will not be able to properly reduce oxygen, and superoxide will be generated. Furthermore, damage to the mitochondrial membrane and a lack of ATP will cause the MPTP to begin to leak free radicals stored within the mitochondria into the extracellular spaces [*Yellon et al., 2007]*.

ROS generation also can compromise the function of the Ca-ATPase on the sarcoplasmic reticulum. Normally, the Ca-ATPase maintains calcium homeostasis in the cardiomyocytes in order to properly allow the ventricles to contract and relax. A decrease in ATP, as well as damage to the transporter from ROS generation, causes a dysregulation of calcium ion management in the cytosolic space, causing a calcium overloaded environment. This excess calcium may partly explain the increase in LVEDP and LVESP in our experiment. The excess calcium ions will prevent the ventricle from fully relaxing, preventing a pressure low enough for the ventricle to fill with blood and increasing the LVEDP. Furthermore, the contractile ability of the heart will be impaired due to low ATP and high calcium, thus decreasing the forward flow of blood and increasing the LVESP. Left ventricular pressures are observed to immediately increase at the time of reperfusion and steadily rise as reperfusion continues. We observed a baseline left ventricular mean pressure of 74.40 mmHg prior to infarction. At the time of reperfusion, the mean LVESP gradually increased, with a mean initial LVESP at 5 minutes reperfusion of 102.91 mmHg and a final LVESP mean of 107.42 mmHg. We observed similar results in the four rat heart trials for LVEDP. The initial mean LVEDP, before infarction, was 4.55 mmHg, which is consistent with a healthy LVEDP in rats. During reperfusion, the LVEDP drastically increased, with a mean initial LVEDP of 95.86 mmHg and a mean end LVEDP of 67.95 mmHg.

6.3.2 Coronary Flow

Blood flow through the coronary vessels occurs during diastole, and in rats typically ranges from 10-15ml/min depending on the oxygen demand of the heart. In MIR, the diastolic blood flow to the coronary arteries may decrease due to a variety of reasons. One major cause is due to endothelial nitric oxide synthase (eNOS). The activation of eNOS has been directly correlated

with coronary diameter [*Toda et al., 2011*], and its function is to increase to availability of nitric oxide to allow for vasodilation. The inactivation of this channel may occur in MIR injury, due to ROS induced phosphorylation of Ser1177, and the result is a reduced amount of NO available to the coronary arteries and eventual vasoconstriction [Hoshino et al., 2005].

Another major cause of reduced coronary flow in MIR injury is due to inappropriate handling of calcium. A study by *Kristiansen et al*. concludes that MIR injury affects a channel called Endothelin B by an increased presence of calcium (released in higher amounts from MIR injury from damage to the sarcoplasmic reticulum) and increased basal smooth muscle tone, ultimately causing reduced coronary flow. Another study by *Dagenais et al.* supports this idea by using calcium channel blockers post-MIR injury, and finds that the intervention reduces MIR injury by enhancing coronary artery relaxation.

The baseline mean coronary flow in the experimental MIR group was 12.76 mmHg, but decreased significantly during reperfusion with an initial mean flow of 1.97mmHg at 5 minutes, and a final mean flow of 7.75 mmHg at 45 minutes. While the coronary blood flow never reaches baseline levels after MIR injury, the flow does improve during reperfusion. This may be due to the increased function of eNOS enzymes during reperfusion [Hoshino et al., 2005], and due to the reduction of extracellular calcium concentrations from increased blood flow *[Kristiansen et al, 2017]*.

6.3.3 dP/dT max and min

dP/dT max and min represent the rate of rise of the left ventricular pressure during the isometric contraction stage of the heart cycle, and the rate of relaxation during isometric relaxation, respectively [*Cardiovascular Physiology]*. In rats, the standard range may vary from heart to heart, but it is useful in comparing initial dP/dT before ischemia to final dP/dT after ischemia

because it quantifies the degree of reduction in the contractility and relaxation ability of the heart. This was observed in the experiment, with an average initial dP/dT max of 1932 mmHg. The dP/dT decreased substantially from baseline to reperfusion, with a mean dP/dT at 5 minutes of 130 mmHg. The dP/dT recovered over the course of the 45 minutes reperfusion in all animals, but never reached baseline again in the animals, representing a significant decrease in the ability of the heart to properly contract.

6.4 Calcium handling abnormality during MIR

The reduction in contractility and relaxation may be due to the excessive calcium ion generation that occurs during MIR injury (*Rhodes et al, 2015)*. With impaired handling of the calcium ions in the extracellular space, the heart is not able to adequately relax and allow time for the left ventricle to fill during diastole. One study by *Rhodes et al.* proposes that many physiologic changes in the heart from MIR injury may be explained from changes in calcium-induced contraction and relaxation. The study proposes that MIR alters calcium sensitivity, activates Ca^{2+}-dependent channels, and causes calcium overload. Futhermore, MIR injury decreases Ca^{2+} contraction coupling, a process that is essential in heart relaxation. Decreases in Ca^{2+} contraction coupling prolong diastole and prevent the cooperative binding of intracellular calcium to troponin C.

6.3.4 Heart Rate

The typical heart rate of a rat ranges from 250-450 beats per minute and can vary drastically depending on the stress of the animal as well as normal variances between them *[JHU Species Information]*. The difference between means in the animal groups in the experiment, however, was minimal, with an initial mean heart rate of 263 beats per minute, and an end heart rate of 259 beats per minute. However, multiple variances in heart rate throughout the experiment were

observed, especially at the beginning of reperfusion. For example, the heart rate of experiment 1 rose from 260 bpm to 343 bpm at the start of reperfusion, but steadily decreased as the experiment continued. Heart rate may predict the overall mortality, or duration of hospital stay [*Indolfi et al., 1993]*.

6.4 Infarct size

The generation of ROS, primarily from the mitochondria, also contribute to the final size of the infarct due to the activation of different apoptotic pathways. This is in addition to the impaired ability of the mitochondria to generate ATP, the cellular damage caused by the leakage of free radicals, and the impaired handling of calcium ions from the sarcoplasmic reticulum. Cytochrome C, a pro-apoptotic molecule, will leak from the mitochondria in an MIR injury and ultimately cause local cells to undergo apoptosis, thus increasing the final size of the infarct [*Yellon et al., 2007]*.

6.5 Limitations

6.5.1 Isolated Heart

The isolated heart does not represent an *in vivo* heart due it its lack of innervation and its lack of ability to be affected by several systems, such as the sympathetic, parasympathetic, and RAAS system. This lack of innervation may affect multiple systems, such as the heart rate. The typical heart rate of a live rat ranges from 300-500bpm, however, the isolated rat heart is 263 ± 5 [Ijic, 1996]. Furthermore, the isolated heart is perfused with Kreb's buffer, rather than blood, and will be lacking multiple normal physiologic substances such as insulin. The lack of proper cellular metabolism with insulin may affect the efficiency of the heart [*Aksentijevic et al., 2015*].

6.5.2 LAD Model

The measurement of proper ligation in a small animal, like the mouse, can be difficult due to the small size of the heart and coronary vessels, in addition to the fast heart rate of the animal [*Verdouw et al., 1998]*.

6.6 Future Studies

Future studies will focus on Apelin, an endogenous peptide ligand for the G-protein coupled receptor APJ, which may have a cardioprotective role limiting infarction size after a myocardial infarction by reducing the production of reactive oxygen species. Apelin is an endogenous ligand of the G protein coupled receptor, known as APJ. First discovered in 1998, Apelin is found within multiple human tissues, and is particularly abundant within cardiomyocytes, vascular endothelial cells and adipose tissue [*Chapman et al., 2014*]. Apelin has been proposed to play a role in a multitude of physiologic processes, including limiting free radical formation, stimulation of angiogenesis, and assisting in early cardiac embryologic development. It may have a cardioprotective role post-MI by reducing the final size of tissue infarct [*Wysocka et al., 2019*]. In particular, ML233, is currently the only full APJ receptor agonist discovered. ML233 is a non-peptide, a benefit of which may be increased solubility, increased metabolic stability and better oral availability, which may contribute to usefulness in a clinical application of Apelin. Furthermore, ML233 is found to be very selective and potent (3.7uM) for the APJ receptor, allowing for future study into quantifying the degree of effect from a strong receptor agonist [*Khan et al., 2011*].

VII. Conclusion

Myocardial ischemia reperfusion injury causes compromised cardiac function, lethal cardiac death; reperfusion induced electrical abnormality; and no coronary blood flow in both the isolated heart MIR model and/or the LAD occlusion/reperfusion model.

VIII. Works Cited

1. Achar SA, Kundu S, Norcross WA. Diagnosis of acute coronary syndrome. *American family physician*. 2005;72(1):119. https://www.ncbi.nlm.nih.gov/pubmed/16035692.

2. Aksentijević D, Lewis HR, Shattock MJ. Is rate–pressure product of any use in the isolated rat heart? assessing cardiac 'effort' and oxygen consumption in the langendorff-perfused heart. *Experimental Physiology*. 2016;101(2):282-294. https://physoc.onlinelibrary.wiley.com/doi/abs/10.1113/EP085380. Accessed Jul 30, 2020. doi: 10.1113/EP085380.

3. Chapman NA, Dupré DJ, Rainey JK. The apelin receptor: Physiology, pathology, cell signalling, and ligand modulation of a peptide-activated class A GPCR. *Biochem Cell Biol*. 2014;92(6):431-440. https://www.ncbi.nlm.nih.gov/pmc/articles/PMC4894813/. Accessed Jul 30, 2020. doi: 10.1139/bcb-2014-0072.

4. Hausenloy DJ, Schulz R, Girao H, et al. Mitochondrial ion channels as targets for cardioprotection. *Journal of Cellular and Molecular Medicine*. 2020;24(13):7102-7114. https://onlinelibrary.wiley.com/doi/abs/10.1111/jcmm.15341. Accessed Jul 30, 2020. doi: 10.1111/jcmm.15341.

5. Neri M, Riezzo I, Pascale N, Pomara C, Turillazzi E. Ischemia/reperfusion injury following acute myocardial infarction: A critical issue for clinicians and forensic pathologists. *Mediators Inflamm*. 2017;2017. https://www.ncbi.nlm.nih.gov/pmc/articles/PMC5327760/. Accessed Jul 30, 2020. doi: 10.1155/2017/7018393.

6. Tinker A, Aziz Q, Thomas A. Review. *Review*. 1979;171(1):12-23. https://www.ncbi.nlm.nih.gov/pmc/articles/PMC3874693/.

7. Amanakis G, Kleinbongard P, Heusch G, Skyschally A. Attenuation of ST-segment elevation after ischemic conditioning maneuvers reflects cardioprotection online. *Basic Res Cardiol*. 2019;114(3):22. Accessed Jul 30, 2020. doi: 10.1007/s00395-019-0732-3.

8. Armstrong M, Kerndt CC, Moore RA. Physiology, baroreceptors. In: *StatPearls*. Treasure Island (FL): StatPearls Publishing; 2020. http://www.ncbi.nlm.nih.gov/books/NBK538172/. Accessed Jul 30, 2020.

9. Bruss ZS, Raja A. Physiology, stroke volume. In: *StatPearls*. Treasure Island (FL): StatPearls Publishing; 2020. http://www.ncbi.nlm.nih.gov/books/NBK547686/. Accessed Jul 30, 2020.

10. Dagenais F, Cartier R, Hollmann C, Buluran J. Calcium-channel blockers preserve coronary endothelial reactivity after ischemia-reperfusion. *The Annals of Thoracic Surgery*. 1997;63(4):1050. http://ats.ctsnetjournals.org/cgi/content/abstract/63/4/1050. Accessed Jul 30, 2020.

11. Fountain JH, Lappin SL. Physiology, renin angiotensin system. In: *StatPearls*. Treasure Island (FL): StatPearls Publishing; 2020. http://www.ncbi.nlm.nih.gov/books/NBK470410/. Accessed Jul 30, 2020.

12. Garcia-Dorado D, Ruiz-Meana M, Piper HM. Lethal reperfusion injury in acute myocardial infarction: Facts and unresolved issues. *Cardiovasc Res*. 2009;83(2):165-168. Accessed Jul 30, 2020. doi: 10.1093/cvr/cvp185.

13. Hoshino S, Kikuchi Y, Nakajima M, et al. Endothelial NO synthase (eNOS) phosphorylation regulates coronary diameter during ischemia-reperfusion in association with oxidative stress. *Free Radical Research*. 2005;39(5):481-489. https://doi.org/10.1080/10715760500073840. Accessed Jul 30, 2020. doi: 10.1080/10715760500073840.

14. Igić R. The isolated perfused "working" rat heart: A new method. *Journal of Pharmacological and Toxicological Methods*. 1996;35(2):63-67. http://www.sciencedirect.com/science/article/pii/1056871996000019. Accessed Jul 30, 2020. doi: 10.1016/1056-8719(96)00001-9.

15. Indolfi C, Ross J. The role of heart rate in myocardial ischemia and infarction: Implications of myocardial perfusion-contraction matching. *Progress in Cardiovascular Diseases*. 1993;36(1):61-74. http://www.sciencedirect.com/science/article/pii/0033062093900226. Accessed Jul 30, 2020. doi: 10.1016/0033-0620(93)90022-6.

16. Kelle S, Roes SD, Klein C, et al. Prognostic value of myocardial infarct size and contractile reserve using magnetic resonance imaging. *J Am Coll Cardiol*. 2009;54(19):1770-1777. Accessed Jul 30, 2020. doi: 10.1016/j.jacc.2009.07.027.

17. Khan P, Maloney PR, Hedrick M, et al. Functional agonists of the apelin (APJ) receptor. In: *Probe reports from the NIH molecular libraries program*. Bethesda (MD): National Center for Biotechnology Information (US); 2010. http://www.ncbi.nlm.nih.gov/books/NBK98921/. Accessed Jul 30, 2020.

18. Kristiansen SB, Haanes KA, Sheykhzade M, Edvinsson L. Endothelin receptor mediated Ca2+ signaling in coronary arteries after experimentally induced ischemia/reperfusion injury in rat. *Journal of Molecular and Cellular Cardiology*. 2017;111:1-9. http://www.sciencedirect.com/science/article/pii/S0022282817301670. Accessed Jul 30, 2020. doi: 10.1016/j.yjmcc.2017.07.013.

19. Mielniczuk LM, Lamas GA, Flaker GC, et al. Left ventricular end-diastolic pressure and risk of subsequent heart failure in patients following an acute myocardial infarction. *Congest Heart Fail*. 2007;13(4):209-214. Accessed Jul 30, 2020. doi: 10.1111/j.1527-5299.2007.06624.x.

20. Ogobuiro I, Wehrle CJ, Tuma F. Anatomy, thorax, heart coronary arteries. In: *StatPearls*. Treasure Island (FL): StatPearls Publishing; 2020. http://www.ncbi.nlm.nih.gov/books/NBK534790/. Accessed Jul 30, 2020.

21. Ong S, Samangouei P, Kalkhoran SB, Hausenloy DJ. The mitochondrial permeability transition pore and its role in myocardial ischemia reperfusion injury. *J Mol Cell Cardiol*. 2015;78:23-34. Accessed Jul 30, 2020. doi: 10.1016/j.yjmcc.2014.11.005.

22. Rhodes SS, Camara AKS, Aldakkak M, Heisner JS, Stowe DF. Stretch-induced increase in cardiac contractility is independent of myocyte Ca2+ while block of stretch channels by streptomycin improves contractility after ischemic stunning. *Physiological Reports*. 2015;3(8):e12486-n/a. https://onlinelibrary.wiley.com/doi/abs/10.14814/phy2.12486. doi: 10.14814/phy2.12486.

23. Toda N, Tanabe S, Nakanishi S. Nitric oxide-mediated coronary flow regulation in patients with coronary artery disease: Recent advances. *International Journal of Angiology*. 2011;20(3):121-134. http://dx.doi.org/10.1055/s-0031-1283220. doi: 10.1055/s-0031-1283220.

24. Van Allen NR, Krafft PR, Leitzke AS, Applegate 2, Richard L, Tang J, Zhang JH. The role of volatile anesthetics in cardioprotection: A systematic review. *Medical gas research*. 2012;2(1):22. https://www.ncbi.nlm.nih.gov/pubmed/22929111. doi: 10.1186/2045-9912-2-22.

25. Verdouw PD, van den Doel, Mirella A., de Zeeuw S, Duncker DJ. Animal models in the study of myocardial ischaemia and ischaemic syndromes. *Cardiovasc Res*. 1998;39(1):121-135. https://academic.oup.com/cardiovascres/article/39/1/121/271944. Accessed Jul 30, 2020. doi: 10.1016/S0008-6363(98)00069-8.

26. Wysocka MB, Pietraszek-Gremplewicz K, Nowak D. The role of apelin in cardiovascular diseases, obesity and cancer. *Frontiers in physiology*. 2018;9:557. https://search.datacite.org/works/10.3389/fphys.2018.00557. doi: 10.3389/fphys.2018.00557.

27. Yellon DM, Hausenloy DJ. Myocardial reperfusion injury. *N Engl J Med*. 2007;357(11):1121-1135. Accessed Jul 30, 2020. doi: 10.1056/NEJMra071667.

28. Klabunde, R. E. (2012). Cardiovascular physiology concepts. Philadelphia, PA: Lippincott Williams & Wilkins/Wolters Kluwer.